University of Amsterdam
Vrije Universiteit Amsterdam

Theoretical Physics (joint degree)

Master's Thesis

Sommerfeld Enhancement in Bound State Dark Matter

Author:
J. H. Streuer

Supervisor:
dr. M. Postma

Secondary Examinor:
dr. C. Weniger

A thesis submitted in fulfillment of the requirements for the degree of MSc

in the

Nikhef Theory Group

July 27, 2017

Abstract

Sommerfeld Enhancement in Bound State Dark Matter

by J. H. Streuer

Despite the strong astrophysical and cosmological evidence for the existence of Dark Matter (DM), its nature is still unresolved. Many models have been constructed in which the current DM density is reproduced as a thermal relic of the evolution of the early universe. The present DM abundance depends sensitively on the annihilation rate. If DM interacts via a light mediator, this annihilation rate can be strongly enhanced through the so-called Sommerfeld Enhancement. In scenarios where the Sommerfeld enhancement is relevant, the formation of DM bound-states should also be taken into account for precise predictions, but is often neglected. These effects can have a big impact on the possible parameter space of many DM models.

This thesis reviews the calculation of the DM relic density, including the effects of Sommerfeld enhancement and bound state formation. We present both numerical and approximate analytical solutions to the set of Boltzmann equations that govern the evolution of DM density, and fit the model parameters such that the observed value for the relic density is matched.

Furthermore, we extend the calculation to the case where DM interacts through a Yukawa potential. Such scenarios are of great interest as they appear naturally in models where DM is charged under the electroweak interactions, such as in supersymmetric extensions of the Standard Model.

Acknowledgements

I would like to thank Marieke Postma and Jordy de Vries for supervising my research. I would like to thank Christoph Weniger for being my secondary corrector. Special thanks to Nikhef for being a great research institution.

"The Universe... What a concept."
-Dr. Jimes Tooper

Contents

Chapter 1

Introduction

1.1 Rotation Curves

The discrepancy between the observed rotation curve of galaxies and the prediction from theory is one of the most famous open problems in physics. The problem itself lies at the boundary of what we know about Newtonian dynamics, which is a limit of Einsteins theory of general relativity.
The first proposal for a dark matter component was by Fritz Zwicky in 1933[1, 2], who used the virial theorem to explain the unexpected velocities of galaxies in the Coma cluster by considering cold non-luminous matter. Similar observations were also made in the Virgo Cluster and the Local group.

Kepler's Third Law of Planetary Motion tells us that the velocity of a rotating object is

$$v_{\mathrm{rot}} = \sqrt{\frac{GM_{\mathrm{encl}}}{r}} \quad , \tag{1.1}$$

where M_{encl} is the mass enclosed within the sphere of radius r centered around the center of mass. Outside of the galactic disk the enclosed mass should remain completely constant if it consisted of only the visible baryonic mass, and the velocity as a function of distance should decrease as the inverse of the square root.
Contrary to this hypothesis, many measurements of the rotation curves of galaxies are not fitted by this relation[3]. Instead, the rotational velocity becomes constant at larger distances, seemingly indicating that the enclosed mass does not become constant at large radii (e.g. beyond the baryonic matter), but rather scales as $M_{\mathrm{encl}}(r) \propto r$. Consequently the mass density at radius r then is

$$\rho(r) = \lim_{\delta r \to 0} \frac{M_{\mathrm{encl}}(r+\delta r) - M_{\mathrm{encl}}(r)}{\frac{4}{3}\pi((r+\delta r)^3 - r^3)} = \frac{M'_{\mathrm{encl}}(r)}{4\pi r^2} \quad , \tag{1.2}$$

$$\int \mathrm{d}^3\boldsymbol{r}\,\rho(r) = 4\pi \int_0^r \rho(r')r'^2 dr' = M_{\mathrm{encl}}(r) \quad , \tag{1.3}$$

where M'_{encl} is the derivative of the enclosed mass with respect to r, which is a constant when $M_{\mathrm{encl}}(r) \propto r$.
This is a good indicator that the Standard Model might be incomplete, and lacks certain particles which do not interact electromagnetically. These particles make up what is called Dark Matter and would be present in every galaxy, or any other large scale structure, dressing it with a so-called dark matter halo, centered at the nucleus of the galaxy, but expanding far beyond the edge of the baryonic disk.

1.2 Detection and Relic Density

The most common dark matter theories consider a (class of) particle(s) which can interact with each other and possibly annihilate into standard model particles. Experiments to detect dark matter can thus be approached in three different ways (see figure 1.1). Scattering experiments, such as Xenon1T, LUX, and PandaX attempt to detect a momentum exchange between standard model particles (Xenon nuclei) and the invisible dark matter. Experiments such as Fermi-LAT and AMS-02 try to detect dark matter indirectly by scanning for rare events of high energy radiation without any other known origin. These high energy gamma rays might originate from a dark matter annihilation. The production of dark matter would happen in collider experiments, such as LHC. Whenever dark matter is produced in a collider we expect to see an energy defect, as the dark mater will have left the collider without interacting. The missing energy and momentum can then be used to determine what mass the dark matter would have had.

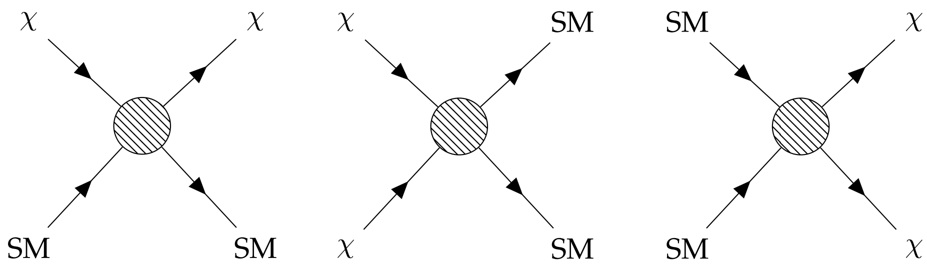

(A) Direct detection (B) Indirect detection (C) Production

FIGURE 1.1: Different procedures for dark matter detection[4]

Chapter 2

The Early Universe

The most widely accepted cosmological model, sometimes referred to as the standard model of cosmology, is the ΛCMD parametrization. It includes a dark energy parameter in the form of a cosmological constant Λ, and a Cold Dark Matter component. Cold dark matter, also known as thermal relic dark matter, is highly dependent on the thermal history of the universe. In the Big Bang scenario, the dark matter particles are created symmetrically, i.e. with the same amount of particles as anti-particles. As the universe cools down it is theorized that there are leftover dark matter particles spread across the universe, unable to find a partner to annihilate with.

2.1 Conservation of Entropy

At early times, the universe was homogeneous and isotropic, so the metric is the Friedman-Lemaître-Robertson-Walker (FLRW) metric. Matter in such a universe resembles an ideal fluid, and can be modeled as such. Even today, this is still a valid approximation for calculations on a cosmological scale. The energy-momentum tensor of a perfect fluid is

$$T_{\mu\nu} = (\rho + p)U_\mu U_\nu + p g_{\mu\nu} \quad , \tag{2.1}$$

where U_μ is the velocity of the fluid, and $g_{\mu\nu}$ is the FLRW metric.

$$\begin{aligned} \mathrm{d}s^2 &= -\mathrm{d}t^2 + a^2(t)\mathrm{d}\mathbf{\Sigma}^2 \\ \Rightarrow g_{\mu\nu} &= \mathrm{diag}(-1, \frac{1}{a^2(t)}, \frac{1}{a^2(t)}, \frac{1}{a^2(t)}) \end{aligned}$$

The scale factor $a(t)$ dictates how the spatial dimensions dilate relative to the temporal dimensions. One of the things it is responsible for is the red-shift of light created a long time ago. In the rest frame of the fluid $U^\mu = (1, \mathbf{0})$. We thus have

$$T^{\mu\nu} = \mathrm{diag}(\rho, \frac{p}{a^2(t)}, \frac{p}{a^2(t)}, \frac{p}{a^2(t)}) \quad . \tag{2.2}$$

Conservation of energy-momentum tensor ($\nabla_\mu T^{\mu 0} = 0$) then gives the continuity equation,

$$\dot{\rho} + 3H(\rho + p) = 0 \quad , \tag{2.3}$$

where $H = \frac{\dot{a}(t)}{a(t)}$ is the Hubble Parameter, which gives a first order rate of expansion.

To determine the change of entropy S over time we consider the second law of thermodynamics. The second law of thermodynamics gives the dependence of entropy on the change in heat of a system. Since our universe has only cooled down since the Big Bang, temperature T is a monotonically decreasing function of time t, and can thus be used a governing evolution parameter instead. When the second law is applied to a comoving volume element in thermal equilibrium, it dictates that

$$\mathrm{d}S = \frac{1}{T}(\mathrm{d}(\rho V) + p\mathrm{d}V) \quad . \tag{2.4}$$

We can also write this as

$$\mathrm{d}S = \frac{1}{T}(\mathrm{d}(V(\rho + p)) - V\mathrm{d}p) \quad . \tag{2.5}$$

Per infinitesimal amount of time this is

$$\begin{aligned} \frac{\mathrm{d}S}{\mathrm{d}t} &= \frac{1}{T}\left(\frac{\mathrm{d}(V(\rho+p))}{\mathrm{d}t} - V\frac{\mathrm{d}p}{\mathrm{d}t}\right) &(2.6)\\ &= \frac{V}{T}\frac{\mathrm{d}\rho}{\mathrm{d}t} + \frac{\rho+p}{T}\frac{\mathrm{d}V}{\mathrm{d}t} &(2.7)\\ &= \frac{V}{T}(\dot{\rho} + 3H(\rho+p)) = 0 \quad , &(2.8) \end{aligned}$$

proving that entropy is conserved for a perfect fluid. We have used that any volume V depends cubically on $a(t)$, so that

$$\begin{aligned} \frac{\mathrm{d}V}{\mathrm{d}t} &\sim \frac{\mathrm{d}}{\mathrm{d}t}a^3(t) \\ &\sim 3\dot{a}(t)a^2(t) \\ &= 3HV \quad . \end{aligned}$$

2.1.1 Entropy density

Starting from equation 2.5 we can also now write

$$\begin{aligned} \frac{\mathrm{d}S}{\mathrm{d}T} &= \frac{1}{T}\frac{\mathrm{d}(V(\rho+p))}{\mathrm{d}T} - \frac{V}{T}\frac{\mathrm{d}p}{\mathrm{d}T} &(2.9)\\ &= \frac{\mathrm{d}(V\frac{\rho+p}{T})}{\mathrm{d}T} - V(\rho+p)\frac{\mathrm{d}\frac{1}{T}}{\mathrm{d}T} - \frac{V}{T}\frac{\rho+p}{T} &(2.10)\\ &= \frac{\mathrm{d}(V\frac{\rho+p}{T})}{\mathrm{d}T} \quad , &(2.11) \end{aligned}$$

proving that $S = V\frac{\rho+p}{T}$ up to a constant. We can define the entropy density $s = S/V$, such that

$$s = \frac{\rho+p}{T} \quad , \tag{2.12}$$

and

$$\dot{s} = -3Hs \quad . \tag{2.13}$$

The entropy density will prove to be a useful quantity later on, when we attempt to determine the evolution of certain other quantities. The integrability condition

$$\frac{\partial^2 S}{\partial T \partial V} = \frac{\partial^2 S}{\partial V \partial T} \tag{2.14}$$

gives

$$\frac{\mathrm{d}}{\mathrm{d}V}\left(\left.\frac{\mathrm{d}S}{\mathrm{d}T}\right|_V\right)\Bigg|_T = \frac{\mathrm{d}}{\mathrm{d}T}\left(\left.\frac{\mathrm{d}S}{\mathrm{d}V}\right|_T\right)\Bigg|_V \tag{2.15}$$

$$\frac{\mathrm{d}}{\mathrm{d}V}\left(\frac{V}{T}\frac{\mathrm{d}\rho}{\mathrm{d}T}\right)\Bigg|_T = \frac{\mathrm{d}}{\mathrm{d}T}\left(\frac{V}{T}\frac{\mathrm{d}\rho}{\mathrm{d}V} + \frac{\rho+p}{T}\right)\Bigg|_V \tag{2.16}$$

$$\frac{1}{T}\frac{\mathrm{d}\rho}{\mathrm{d}T} = \frac{1}{T}\frac{\mathrm{d}(\rho+p)}{\mathrm{d}T} - \frac{1}{T^2}\left(V\frac{\mathrm{d}\rho}{\mathrm{d}V} + (\rho+p)\right) \tag{2.17}$$

$$\frac{\mathrm{d}p}{\mathrm{d}T} = \frac{\rho+p}{T} + \frac{V}{T}\frac{\mathrm{d}\rho}{\mathrm{d}V} \quad . \tag{2.18}$$

For a homogeneous universe the last term vanishes, since the density is equal in every volume element at fixed times (and thus temperatures). This gives us a way to calculate the entropy density if we know the pressure distribution of the species of particles in question.

2.2 Equilibirum Distributions

To determine the amount of dark matter in our universe we need to know the equilibrium number density. The number density n_a of a relativistic particle of species a with energy $E_a(|\boldsymbol{p}|) = \sqrt{\boldsymbol{p}^2 + m_a^2}$ is given by

$$n_a = g_a \int \frac{\mathrm{d}^3\boldsymbol{p}}{(2\pi)^3} f_a(|\boldsymbol{p}|) \quad , \tag{2.19}$$

where the distribution function, which can either be Bose-Einstein or Fermi-Dirac depending on the statistical nature of a, is

$$f_a(|\boldsymbol{p}|) = \frac{1}{\mathrm{e}^{\frac{E_a(|\boldsymbol{p}|)-\mu_a}{T_a}} \mp 1} \quad , \tag{2.20}$$

in thermal equilibrium. The internal degrees of freedom, such as spin, charge, and color are denoted by g_a. The chemical potential μ_a is mostly ignored in the calculations we present.
In the classical limit the Bose-Einstein and the Fermi Dirac distribution look like the Maxwell-Boltzmann distribution.

$$f_a(|\boldsymbol{p}|) = \mathrm{e}^{-\frac{E_a(|\boldsymbol{p}|)-\mu_a}{T_a}} \tag{2.21}$$

The classical limit is where the quantum nature of the particles vanishes. For high temperatures we automatically have a low occupation number. This is because the amount of accessible high energy states becomes large. Thus the denominator of equation 2.20 must be large, and therefore the ± 1 may be neglected, and we obtain Maxwell-Boltzmann statistics. The physics of higher energy states becoming available with increasing temperature actually lies in $\mu(T)$, which is defined through the partition function.
In cases where the chemical potential is a constant, commonly zero, the opposite takes effect. One can now take the limit of $T \to 0$ directly in 2.20, and find Maxwell-Boltzmann statistics.

We have similar definitions for the energy density and pressure of particle a. They are defined through their expressions in terms of momentum and energy, which are then averaged over all possible momenta, weighted with the distribution function.

$$\rho_a = g_a \int \frac{\mathrm{d}^3\boldsymbol{p}}{(2\pi)^3} f_a(|\boldsymbol{p}|) E_a(|\boldsymbol{p}|) \tag{2.22}$$

$$p_a = g_a \int \frac{\mathrm{d}^3\boldsymbol{p}}{(2\pi)^3} f_a(|\boldsymbol{p}|) \frac{\boldsymbol{p}^2}{3E_a(|\boldsymbol{p}|)} \tag{2.23}$$

2.2.1 Ultra-relativistic limit ($m \ll T_a, |\mathbf{p}|$)

In the ultra-relativistic limit we have $E \approx |\boldsymbol{p}|$, or, equivalently $m \approx 0$, so the integrals become

$$n_a = \frac{g_a}{2\pi^2} \int_0^\infty \mathrm{d}|\boldsymbol{p}||\boldsymbol{p}|^2 f_a(|\boldsymbol{p}|) \quad , \tag{2.24}$$

$$\rho_a = \frac{g_a}{2\pi^2} \int_0^\infty \mathrm{d}|\boldsymbol{p}||\boldsymbol{p}|^3 f_a(|\boldsymbol{p}|) \quad , \tag{2.25}$$

$$p_a = \frac{1}{3}\rho_a \quad . \tag{2.26}$$

To solve these integrals, we first derive the result of some more general integrals. For a Maxwell-Boltzmann distribution we simply get the definition of the gamma function.

$$\int_0^\infty \mathrm{d}x x^n \mathrm{e}^{-x} = \Gamma(n+1) \tag{2.27}$$

The integral over the Bose-Einstein and Fermi-Dirac distributions can be reduced to an integral over the Maxwell-Boltzmann distribution by making use of the Riemann zeta function[1].

$$\int_0^\infty \mathrm{d}x \frac{x^n}{\mathrm{e}^x - 1} = \int_0^\infty \mathrm{d}x x^n \mathrm{e}^{-x} \sum_{k=0}^\infty \mathrm{e}^{-kx} \tag{2.28}$$

$$= \sum_{k=0}^\infty \int_0^\infty \mathrm{d}x x^n \mathrm{e}^{-x(k+1)} \tag{2.29}$$

Changing variables, i.e. $x = \frac{y}{k+1}$, gives

$$\int_0^\infty \mathrm{d}x \frac{x^n}{\mathrm{e}^x - 1} = \sum_{k=0}^\infty \frac{1}{(k+1)^{n+1}} \int_0^\infty \mathrm{d}y y^n \mathrm{e}^{-y} \tag{2.30}$$

$$= \sum_{k=1}^\infty \frac{1}{(k)^{n+1}} \int_0^\infty \mathrm{d}y y^n \mathrm{e}^{-y} \tag{2.31}$$

$$= \zeta(n+1)\Gamma(n+1) \quad . \tag{2.32}$$

[1]Note that the Riemann zeta function $\zeta(s)$ is undefined for $s = 1$. The integral over the Bose-Einstein distribution for $n = 0$ can be calculated to be $\ln(2)$, but the Fermi-Dirac integral is undefined. These two integrals thus only work for $n \in \mathbb{N}_1$.

For the Fermi-Dirac integral we get

$$\int_0^\infty \mathrm{d}x \frac{x^n}{\mathrm{e}^x + 1} = \sum_{k=0}^{\infty} \frac{(-1)^k}{(k+1)^{n+1}} \Gamma(n+1) \tag{2.33}$$

$$= -\sum_{k=1}^{\infty} \frac{(-1)^k}{(k)^{n+1}} \Gamma(n+1) \quad . \tag{2.34}$$

Now note that

$$\sum_{k=1}^{\infty} \frac{(-1)^k}{k^n} + \sum_{k=1}^{\infty} \frac{1}{k^n} = 2 \sum_{k=2,4,6,\ldots} \frac{1}{k^n} \tag{2.35}$$

$$= 2 \sum_{k=1}^{\infty} \frac{1}{(2k)^n} \tag{2.36}$$

$$= 2^{1-n} \sum_{k=1}^{\infty} \frac{1}{k^n} \quad , \tag{2.37}$$

so

$$-\sum_{k=1}^{\infty} \frac{(-1)^k}{(k)^n} = \zeta(n) - 2^{1-n}\zeta(n) \quad , \tag{2.38}$$

and thus

$$\int_0^\infty \mathrm{d}x \frac{x^n}{\mathrm{e}^x + 1} = (1 - 2^{-n})\zeta(n+1)\Gamma(n+1) \quad . \tag{2.39}$$

Applying these results to our integrals for number density, density, and pressure, we get that

$$n_a = \frac{g_a}{\pi^2}\zeta(3) T_a^3 \times \begin{cases} 1 & \text{BE} \\ 3/4 & \text{FD} \\ 1/\zeta(3) & \text{MB} \end{cases} \quad , \tag{2.40}$$

(2.41)

$$\rho_a = \frac{g_a \pi^2}{30} T_a^4 \times \begin{cases} 1 & \text{BE} \\ 7/8 & \text{FD} \\ 1/\zeta(4) & \text{MB} \end{cases} \quad , \tag{2.42}$$

(2.43)

$$p_a = \frac{g_a \pi^2}{90} T_a^4 \times \begin{cases} 1 & \text{BE} \\ 7/8 & \text{FD} \\ 1/\zeta(4) & \text{MB} \end{cases} \quad . \tag{2.44}$$

For convenience we will from here on absorb the three statistical scenarios in g, denoted as $g_a^{(n)}$, $g_a^{(\rho)}$, and $g_a^{(p)}$ (notice that $g_a^{(\rho)}$ and $g_a^{(p)}$ are equal). We can also define $g_*^{(\rho)}$, which is the effective total of degrees of freedom of our universe. It can be defined through the density of the universe as

$$\rho_* = \frac{g_* \pi^2}{30} T_*^4 = \sum_i \rho_i = \sum_i \frac{g_i \pi^2}{30} T_i^4 \quad ,$$
$$\Rightarrow \delta g_* = \frac{30}{\pi^2} \frac{1}{T_*^4} \rho_i \quad .$$

For high temperatures T_i we can solve the integrals of ρ_i easily and use our notation as introduced before to absorb the fermionic and bosonic statistics to get

$$g_*(T_i \gg m_i) = \sum_i g_i^{(\rho)} \frac{T_i^4}{T_*^4} \quad . \tag{2.45}$$

If all the different species are the same temperature, we can simply sum all the degrees of freedom directly, with the fermions having a factor of $\frac{7}{8}$ compared to bosons. For our standard model we then get $g_* = 106.75$[2]. It can be used to compute the total density, pressure, and entropy density of the universe at the time of the Big Bang, when the universe is in equilibrium.

2.2.2 Non-relativistic limit ($T \ll m$)

In the non-relativistic limit the statistics of particle a look like the Maxwell-Boltzmann distribution. We can rewrite the number density integral into a simple Gaussian integral as

$$n_{\mathrm{nr}} = \frac{g_a}{2\pi^2} \int_0^\infty \mathrm{d}|\boldsymbol{p}| |\boldsymbol{p}|^2 \mathrm{e}^{-\sqrt{|\boldsymbol{p}|^2 + m^2}/T_a} \tag{2.46}$$
$$= \frac{g_a}{2\pi^2} \int_0^\infty \mathrm{d}|\boldsymbol{p}| |\boldsymbol{p}|^2 \mathrm{e}^{-(1+\frac{|\boldsymbol{p}|^2}{2m^2})\frac{m}{T_a}} \tag{2.47}$$
$$= -\frac{g_a}{2\pi^2} \mathrm{e}^{-\frac{m}{T_a}} \partial_A \left[\int_0^\infty \mathrm{d}|\boldsymbol{p}| \mathrm{e}^{-A|\boldsymbol{p}|^2} \right] \Bigg|_{A=\frac{1}{2mT_a}} \tag{2.48}$$
$$= -\frac{g_a}{2\pi^2} \mathrm{e}^{-\frac{m}{T_a}} \partial_A \left[\sqrt{\frac{\pi}{A}} \right] \Bigg|_{A=\frac{1}{2mT_a}} \tag{2.49}$$
$$= g_a \left(\frac{m T_a}{2\pi} \right)^{\frac{3}{2}} \mathrm{e}^{-\frac{m}{T_a}} \tag{2.50}$$

$$\rho_{\mathrm{nr}} = m n_{\mathrm{nr}} \quad , \tag{2.51}$$
$$p_{\mathrm{nr}} = T n_{\mathrm{nr}} \quad . \tag{2.52}$$

The energy density ρ_a in this limit has changed to a mass density. As corollary, we can note that in this limit $p_{\mathrm{nr}} \ll \rho_{\mathrm{nr}}$, and that the last equation is the ideal gas law.

2.3 The Hubble Parameter

When we consider dark matter and the evolution of its density in an expanding universe, the annihilation rate is balanced by the Hubble parameter at later times. The

[2]This does not include the dark matter degrees of freedom g_χ and g_φ

dark matter will have trouble annihilating simply because the two particles necessary for this process lie too far apart. This leads to a "relic density" of dark matter, which in the thermal dark matter scenario is the dark matter we observe today. To perform explicit calculations later, we now need to determine exactly what the Hubble parameter $H(T)$ looks like. We start with a radiation dominated universe ($p = \frac{1}{3}\rho$) and solve the Friedmann equations for $\dot{H}$.

$$\dot{H} = -4\pi G(\rho + p) \tag{2.53}$$

$$= -\frac{16\pi}{3}\frac{1}{m_{Pl}^2}\rho \tag{2.54}$$

When we substitute the relativistic solution for the total density of the universe ρ_* (equation 2.42), we find

$$\frac{\mathrm{d}H}{\mathrm{d}t} = -g_*^{(\rho)}\frac{16\pi^3}{90}\frac{T^4}{m_{Pl}^2} \quad . \tag{2.55}$$

We can now change variables from t to T, by making use of what we know about the entropy density s. We get

$$\frac{\mathrm{d}H}{\mathrm{d}T}\frac{\mathrm{d}T}{\mathrm{d}s}\frac{\mathrm{d}s}{\mathrm{d}t} = -g_*^{(\rho)}\frac{16\pi^3}{90}\frac{T^4}{m_{Pl}^2} \tag{2.56}$$

$$\frac{\mathrm{d}H}{\mathrm{d}T} = -g_*^{(\rho)}\frac{16\pi^3}{90}\frac{T^4}{m_{Pl}^2}\cdot\left(\frac{\mathrm{d}s}{\mathrm{d}T}\right)\cdot\left(\frac{\mathrm{d}s}{\mathrm{d}t}\right)^{-1} \tag{2.57}$$

$$\frac{\mathrm{d}H}{\mathrm{d}T} = g_*^{(\rho)}\frac{16\pi^3}{90}\frac{T^4}{m_{Pl}^2}\cdot\left(\frac{\mathrm{d}^2p}{\mathrm{d}T^2}\right)\frac{1}{3Hs} \tag{2.58}$$

$$\frac{\mathrm{d}H}{\mathrm{d}T} = g_*^{(\rho)}\frac{16\pi^3}{90}\frac{1}{m_{Pl}^2}T^3\frac{1}{H} \quad . \tag{2.59}$$

When we assume a power law $H(T) = aT^n$, we find that $\frac{\mathrm{d}H}{\mathrm{d}T} = naT^{n-1} = na^2T^{2n-1}H^{-1}$. We obtain the equation above for $n = 2$, and the value for a follows.

$$H(T) = \sqrt{\frac{8\pi^3}{90}}\frac{1}{m_{Pl}}\sqrt{g_*^{(\rho)}}T^2 \tag{2.60}$$

$$\approx 1.66\frac{1}{m_{Pl}}\sqrt{g_*^{(\rho)}}T^2 \tag{2.61}$$

For the evolution of the dark mater density it is very useful to use $x = m/T$ as a governing parameter. The Hubble parameter is then often written as

$$H(x) = H(m)x^{-2} \quad , \text{ where } H(m) \approx 1.66\sqrt{g_*^{(\rho)}}\frac{m^2}{m_{Pl}} \quad . \tag{2.62}$$

Chapter 3

The Boltzmann Equation

One of the simplest models to consider is a toy model with a $U(1)_{\mathrm{DM}}$ gauge group, similar to the familiar quantum electrodynamics. The dark matter that makes up the thermal relic consists of a Dirac particle and an anti-particle, or alternatively a single Majorana particle which is its own anti-particle. The gauge boson which mediates between these particles, is what is known as a dark photon.
The dark matter can annihilate into dark photons, reducing the number density, and thus the observed density parameter. The dark photons are relativistic when their mass is low, so they do not contribute significantly to the density parameter, similar to the QED photon. It is then finally assumed that these dark photons decay into (relatively) light SM particles and anti-particles.
In such a toy model, we would have an equilibrium between annihilation and creation during and shortly after the big bang. When the universe settles, the channels are thrown off-ballance, and the dark matter particles start decaying into SM particles. At even later times, however, when the universe is cold and dilated, some dark matter will remain as a thermal relic, due to not being able to find an annihilation partner faster than the expansion of the universe.

3.1 S-Channel Annihilation

3.1.1 Boltzmann Equation

The Boltzmann equation in what statistically describes the evolution of a thermodynamic system that is not in equilibrium. Rather than considering every single particle and their positions and momenta, The particles are assumed to lie at an arbitrary point in parameter space, described by their distribution function. The evolution of this distribution is decided by the transport, external forces, and the specific microscopic processes the particles are affected by. The Boltzmann equation for species χ is typically split into two parts,

$$\hat{L}[f_\chi] = \hat{C}[f_\chi] \quad , \tag{3.1}$$

where $\hat{L}$ is the Liouville operator and $\hat{C}$ is the collision operator. The Liouville operator describes the change in energy density both over time and through diffuion, whereas the collision operator is used for non-trivial behavior, such as decay, which changes the total amount of particles. Without interactions, the change in energy density would be caused only by diffusion. In its covariant or GR form the Liouville operator is

$$\hat{L}[f] = E\frac{\partial f}{\partial t} - H|\boldsymbol{p}|^2\frac{\partial f}{\partial E} \quad , \tag{3.2}$$

where we have no diffusion, i.e. derivatives with respect to any spatial dimensions, due to the universe being homogeneous. From this we get

$$g\int \frac{\mathrm{d}^3\boldsymbol{p}}{(2\pi)^3}\frac{\hat{L}[f]}{E} = \dot{n} - Hg\int \frac{d^3\boldsymbol{p}}{(2\pi)^3}\frac{|\boldsymbol{p}|^2}{E}\frac{\partial f}{\partial E} \tag{3.3}$$

$$= \dot{n} - \frac{Hg}{2\pi^2}\int \mathrm{d}|\boldsymbol{p}|\frac{|\boldsymbol{p}|^4}{E}\frac{\partial p}{\partial E}\frac{\partial f}{\partial p} \tag{3.4}$$

$$= \dot{n} - \frac{Hg}{2\pi^2}\int \mathrm{d}|\boldsymbol{p}||\boldsymbol{p}|^3\frac{\partial f}{\partial p} \tag{3.5}$$

$$= \dot{n} + 3Hn \tag{3.6}$$

$$= g\int \frac{\mathrm{d}^3\boldsymbol{p}}{(2\pi)^3}\frac{\hat{C}[f]}{E} \quad . \tag{3.7}$$

Collision Operator

The collision operator gives the rate at which the energy density changes due to interaction processes. When we know everything about the initial state particles, the rate of change would simply be $E\Gamma = E\sigma v n$, where σ is the classical cross-section. The quantity σv in this case would simply give the volume that a particle covers per unit of time. When multiplied with n, the average amount of particles per volume, this then gives the average amount of particle encounters per unit of time. If our particles annihilate when they touch, Γ is then the annihilation rate of our species.
In Boltzmann's picture, however, we don't know anything but the distribution function of our species, and therefore we must average over all of phase space. Moreover, since we are accounting for quantum mechanical processes, we express the transition rate in terms of Feynman invariant amplitudes. We then end up with

$$g_\chi\int \frac{\mathrm{d}^3\boldsymbol{p}_\chi}{(2\pi)^3}\frac{\hat{C}[f_\chi]}{E_\chi} = -\int \mathrm{d}\Pi_\chi \mathrm{d}\Pi_a d\Pi_b\cdots \mathrm{d}\Pi_i \mathrm{d}\Pi_j\cdots \tag{3.8}$$

$$\times\,(2\pi)^4\delta^4(p_\chi + p_a + p_b\cdots - p_i - p_j\cdots) \tag{3.9}$$

$$\times\,\left[|\mathcal{M}|^2_{\chi+a+b\cdots\to i+j\cdots} f_\chi f_a f_b\cdots(1\pm f_i)(1\pm f_j)\cdots\right. \tag{3.10}$$

$$\left. -\,|\mathcal{M}|^2_{i+j\cdots\to\chi+a+b\cdots} f_i f_j\cdots(1\pm f_\chi)(1\pm f_a)(1\pm f_b)\cdots\right] \quad , \tag{3.11}$$

where we have for simplicity denoted only two interaction channels, namely that of $\chi + a + b\cdots \to i + j\cdots$ and its inverse process. The differentials $\mathrm{d}\Pi = \frac{g}{(2\pi)^3}\frac{\mathrm{d}^3\boldsymbol{p}}{2E}$ denote an integral over Lorentz invariant phase-space (LIPS). The factors of $(1\pm f)$ correspond to Bose-Enhancement and Pauli blocking, which can be neglected in our case, since for the major part of the evolution of our universe, it is very cold, and for $T_i \to 0$ we have $f_i \ll 1$. The Bose enhancement and Pauli blocking are only relevant right after the Big Bang, when temperatures are still high. But because of the principle of detailed balance we know that all processes cancel each other in equilibrium, and thus we can pretend the collision term is effectively zero anyway. Since it is not until after the dark matter is no longer in thermal equilibrium with the rest of the universe, we can assume that all species under the integral whose statistics do not concern us are in thermal equilibrium. When the universe is cold, their statistics become Maxwell-Boltzmann. The Feynman invariant amplitudes $|\mathcal{M}|^2$ include all statistical factors and are spin averaged. Furthermore, they obey CP invariance.

Therefore we have

$$\dot{n}_\chi + 3Hn_\chi = -\int \mathrm{dLIPS}(2\pi)^4\delta^4(p_\chi + p_a + p_b \cdots - p_i - p_j \cdots) \tag{3.12}$$

$$\times |\mathcal{M}|^2_{\chi+a+b\cdots\to i+j\cdots} [f_\chi f_a f_b \cdots - f_i f_j \cdots] \quad . \tag{3.13}$$

We can further improve on this equation by noticing that the product of all equilibrium distributions $f_i^{\mathrm{EQ}} f_j^{\mathrm{EQ}} \cdots$ using energy conservation is exactly equal to $f_\chi^{\mathrm{EQ}} f_a^{EQ} f_b^{EQ} \cdots$ when temperatures are low. For a system where only $\chi\bar{\chi} \to X\bar{X}$ and its inverse process takes place, we get

$$\dot{n}_\chi + 3Hn_\chi = -\int \mathrm{dLIPS}(2\pi)^4\delta^4(p_\chi + p_{\bar{\chi}} - p_X - p_{\bar{X}}) \tag{3.14}$$

$$\times |\mathcal{M}|^2_{\chi\bar{\chi}\to X\bar{X}} \left[f_\chi f_{\bar{\chi}} - f_\chi^{\mathrm{EQ}} f_{\bar{\chi}}^{\mathrm{EQ}}\right] \quad . \tag{3.15}$$

We can now write $f_\chi = \frac{n_\chi}{n_\chi^{\mathrm{EQ}}} f_\chi^{\mathrm{EQ}}$, to absorb all non-equilibrium behavior of χ into n_χ, which is no longer energy dependent. We can then pull those factors of n out of the integral to arrive at

$$\dot{n}_\chi + 3Hn_\chi = -\left[n_\chi n_{\bar{\chi}} - n_\chi^{\mathrm{EQ}} n_{\bar{\chi}}^{\mathrm{EQ}}\right] \frac{1}{n_\chi^{\mathrm{EQ}} n_{\bar{\chi}}^{\mathrm{EQ}}} \int \mathrm{dLIPS}(2\pi)^4\delta^4(p_\chi + p_{\bar{\chi}} - p_X - p_{\bar{X}}) \tag{3.16}$$

$$\times |\mathcal{M}|^2_{\chi\bar{\chi}\to X\bar{X}} f_\chi^{\mathrm{EQ}} f_{\bar{\chi}}^{\mathrm{EQ}} \tag{3.17}$$

$$= -\left[n_\chi n_{\bar{\chi}} - n_\chi^{\mathrm{EQ}} n_{\bar{\chi}}^{\mathrm{EQ}}\right] \langle \sigma_{\chi\bar{\chi}\to X\bar{X}} |v| \rangle \quad . \tag{3.18}$$

We should now consider what differs between the scenario in which the darkmatter is its own anti-particle (i.e. when we are speaking of real scalars or Majorana fermions) and the one in which it is not (i.e. complex scalars or Dirac fermions). If there is a particle as well as an anti-particle component to dark matter, we can leave our Boltzmann equation as is. We should later on add a factor of 2 when calculating the relic density $\Omega_{\chi\bar{\chi}}$, as the antiparticles also count as dark matter.
When we only have one type of dark matter particle, we should add a factor of 2 to our Boltzmann equation to account for the simultaneous annihilation/creation of two dark matter particles. However, due to combinatorics we get an additional symmetry factor of $\frac{1}{2}$ from our Feynman diagrams. Usually this factor would be absorbed in the coupling constant in the Lagrangian as $\lambda\phi^n \to \frac{\lambda'}{n!}\phi^n$ to make the combinatorics in higher order diagrams easier. With this prescription we find that Feynman amplitudes have a factor of $\frac{1}{2}$ for each interaction vertex.

We now consider symmetric dark matter ($n_\chi = n_{\bar{\chi}}$). For convenience we can normalize n with the entropy density $s = S/a^3$ to get a comoving volume independent quantity $Y = n/s$. We then have

$$s\dot{Y}_\chi = \frac{\mathrm{d}}{\mathrm{d}t}(sY_\chi) - Y_\chi \dot{s} \tag{3.19}$$

$$= \dot{n_\chi} - Y_\chi(-3Hs) \tag{3.20}$$

$$= \dot{n_\chi} + 3Hn_\chi \tag{3.21}$$

$$= -\langle \sigma |\boldsymbol{v}| \rangle [n_\chi^2 - (n_\chi^{\mathrm{EQ}})^2] \quad , \tag{3.22}$$

and thus

$$\dot{Y}_\chi = -s\langle\sigma|\boldsymbol{v}|\rangle[Y_\chi^2 - (Y_\chi^{\mathrm{EQ}})^2] \quad . \tag{3.23}$$

It is useful and customary to now write our Boltzmann equation in terms of $x = m_\chi/T$. We use

$$\begin{aligned}\frac{\mathrm{d}x}{\mathrm{d}t} &= \frac{\mathrm{d}x}{\mathrm{d}T}\frac{\mathrm{d}T}{\mathrm{d}s}\frac{\mathrm{d}s}{\mathrm{d}t} \\ &= \frac{m_\chi}{T^2}\left(\frac{3s}{t}\right)(-3Hs) \\ &= Hx \quad ,\end{aligned}$$

to finally get

$$\begin{aligned}\frac{\mathrm{d}Y_\chi}{\mathrm{d}x} &= -\frac{s\langle\sigma|\boldsymbol{v}|\rangle}{xH}[Y_\chi^2 - (Y_\chi^{\mathrm{EQ}})^2] && (3.24)\\ \Bigg(\quad &= -\frac{Y_\chi^{\mathrm{EQ}}}{x}\frac{\Gamma_\chi}{H}\left[\left(\frac{Y_\chi}{Y_\chi^{\mathrm{EQ}}}\right)^2 - 1\right]\Bigg) && (3.25)\\ &= -\frac{\langle\sigma|\boldsymbol{v}|\rangle}{xH}\frac{\mathrm{d}p}{\mathrm{d}T}[Y_\chi^2 - (Y_\chi^{\mathrm{EQ}})^2] && (3.26)\\ &= -\frac{\lambda}{x^2}[Y_\chi^2 - (Y_\chi^{\mathrm{EQ}})^2] \quad , && (3.27)\end{aligned}$$

where

$$\lambda = \sqrt{\frac{\pi}{45}}\frac{g_*^{(p)}}{\sqrt{g_*^{(\rho)}}}m_\chi m_{Pl}\langle\sigma|\boldsymbol{v}|\rangle \quad , \tag{3.28}$$

$$Y_\chi^{\mathrm{EQ}} = \frac{n_\chi^{\mathrm{EQ}}}{s} = \frac{90}{(2\pi)^{7/2}}\frac{g_\chi}{g_*^{(p)}}x^{3/2}\mathrm{e}^{-x} \quad , \tag{3.29}$$

and for s-channel decay $\langle\sigma|\boldsymbol{v}|\rangle \sim \sigma_0 = \pi\frac{\alpha^2}{m^2}$.

Equation 3.25 shows nicely how the amount of dark matter is governed by the balance between the annihilation rate and the expansion of the universe. At a certain time x_f the dark mater density will be too low for the dark matter to find a partner to annihilate with due to the expansion of the universe. This is called the freeze-out time. For some period $1 \leq x \leq x_f$, Y_χ tracks Y_χ^{EQ} as it comes out of the equilibrium at $x = 1$, but around $x = x_f$ this stops. At times larger than x_f the density won't change much anymore because the universe simply expands faster than the dark matter particles can find each other.

After freeze-out Y_χ remains approximately constant, meaning that n_χ changes the same way s does, which is purely due to the expansion of the universe. The dark matter particles can still communicate with the dark photons of the thermal bath, and are thus in thermal equilibrium. Until the dark mater particles no longer transfer momentum among themselves or travel long distances, they could still find a partner and annihilate. The point at which the dark matter decouples kinetically from the thermal bath is obtained by solving $H(T_{\mathrm{kd}}) \sim n_\chi(T_{\mathrm{kd}})\sigma_0\frac{T_{\mathrm{kd}}}{m_\chi}$[5], i.e. when the momentum transfer rate is less than the expansion of the universe. This then gives that the kinetic decoupling is of the order

$$x_{\mathrm{kd}} \sim 10^7 \alpha \sqrt{\frac{\mathrm{TeV}}{m_\chi}} \quad , \tag{3.30}$$

and at this point we are confident that Y_χ and $N_\chi = n_\chi V$ are constant, even if a certain annihilation process becomes more likely to occur at low temperatures.

The Boltzmann equation we have arrived at is a particular version of the Riccati eqaution. The equation has no exact solution and must be solved numerically, or approximated.

3.1.2 Approximate solution

For an approximate as well as a numerical solution the substitution $\Delta_\chi(x) = Y_\chi(x) - Y_\chi^{\mathrm{EQ}}(x)$ makes sense[1]. We end up with

$$\frac{\mathrm{d}\Delta_\chi}{\mathrm{d}x} = -\frac{\mathrm{d}Y_\chi^{\mathrm{EQ}}}{\mathrm{d}x} - \frac{\lambda}{x^2}\left[\Delta_\chi^2 + 2\Delta_\chi Y_\chi^{\mathrm{EQ}}\right] \quad , \tag{3.31}$$

which we can now solve numerically or treat analytically in different limits. For $1 \leq x \leq x_f$ we know that Δ_χ and $\frac{\mathrm{d}\Delta_\chi}{\mathrm{d}x}$ are negligible, because Y_χ is tracking Y_χ^{EQ}. We get

$$\Delta_\chi(x) = \frac{x^2}{2\lambda} \quad \text{for} \quad 1 \leq x \leq x_f \quad . \tag{3.32}$$

For $x_f \ll x$ we know that Y_χ^{EQ} is negligible and get

$$\frac{\mathrm{d}\Delta_\chi}{\mathrm{d}x} = -\frac{\lambda}{x^2}\Delta_\chi^2 \quad , \tag{3.33}$$

$$\int_{x_f}^{x} \frac{1}{\Delta_\chi^2}\mathrm{d}\Delta_\chi = -\int_{x_f}^{x} \frac{\lambda}{x^2}\mathrm{d}x \quad , \tag{3.34}$$

$$\Delta_\chi(x) = \frac{1}{\frac{\lambda}{x_f} - \frac{\lambda}{x} + \frac{1}{\Delta_\chi(x_f)}} \quad \text{for} \quad x_f \leq x \quad , \tag{3.35}$$

$$\Delta_\chi \underset{x\to\infty}{=} \frac{x_f^2}{\lambda(x_f+2)} \quad . \tag{3.36}$$

The freeze-out time x_f is the time at which Y_χ starts to diverge significantly from Y_χ^{EQ}. We can formally define it through $\Delta_\chi(x_f) = cY_\chi^{\mathrm{EQ}}(x_f)$, where c is a constant of order 1, later chosen such that equation 3.36 fits the result from a numerical solution to the Boltzmann equation. At $x = x_f$ the Boltzmann equation turns into an expression for the freeze-out time.

$$\frac{x_f^2}{Y_\chi^{\mathrm{EQ}}} = \lambda c(c+2) \quad . \tag{3.37}$$

[1] This substitution is not at all necessary for an analytic approximation and can be worked around, but for most numerical calculations using a computer it is a must. It is adopted here as a convention/tradition because of how often it has been used in literature.

This then gives

$$\sqrt{x_f}\mathrm{e}^{x_f} = \frac{1}{4\pi^3}\sqrt{\frac{45}{2}} m_\chi m_{\mathrm{Pl}} \sigma_0 \frac{g_\chi}{\sqrt{g_*^{(\rho)}}} c(c+2) \quad . \tag{3.38}$$

As it turns out, $c(c+2) \approx 1$ is a good fit[6], and this gives a freeze-out time of

$$x_f + \frac{1}{2}\ln x_f = \ln\left(\frac{\sqrt{\frac{45}{2}}}{4\pi^2}\frac{g_\chi}{\sqrt{g_*^{(\rho)}}}\frac{m_{\mathrm{Pl}}}{m}\alpha^2\right) \tag{3.39}$$

$$x_f \approx \ln\left(0.12\frac{g_\chi}{\sqrt{g_*^{(\rho)}}}\frac{m_{\mathrm{Pl}}}{m}\alpha^2\right) - \frac{1}{2}\ln\ln\left(0.12\frac{g_\chi}{\sqrt{g_*^{(\rho)}}}\frac{m_{\mathrm{Pl}}}{m}\alpha^2\right) \quad . \tag{3.40}$$

The value of c needs to be determined only once, since equation 3.38 can be re-derived for more general cases, but will always have the same c dependency. For values of α and m_χ that reproduce the experimentally observed dark matter relic density, typically $x_f \approx 25$.

3.1.3 On the fit parameter $c(c+2)$

Consider a Boltzmann equation with multiple annihilation channels $\frac{\lambda_i(x)}{x^2}Y_\chi^2$ and creation channels $F_j(x)$, such that all these decays and formation processes balance each other in equilibrium. The Boltzmann equation can then be written as

$$\frac{\mathrm{d}Y_\chi}{\mathrm{d}x} = -\frac{\sum_i \lambda_i(x)}{x^2}Y_\chi^2 + \sum_j F_j(x) \quad , \tag{3.41}$$

and for early times $\frac{\mathrm{d}\Delta_\chi}{\mathrm{d}x} = 0$ or $\frac{\mathrm{d}Y_\chi}{\mathrm{d}x} = \frac{\mathrm{d}Y_\chi^{\mathrm{EQ}}}{\mathrm{d}x}$, so

$$\frac{\mathrm{d}Y_\chi^{\mathrm{EQ}}}{\mathrm{d}x} = -\frac{\sum_i \lambda_i(x)}{x^2}Y_\chi^2 + \sum_j F_j(x) \quad . \tag{3.42}$$

Now, as the universe comes out of equilibrium, we still have our creation channels compensating our annihilation channels, so

$$\frac{\sum_i \lambda_i(x)}{x^2}(Y_\chi^{\mathrm{EQ}})^2 = \sum_j F_j(x) \quad \text{for} \quad 1 < x < x_f \quad , \tag{3.43}$$

which is known as the principle of detailed balance. This gives us

$$\frac{\mathrm{d}Y_\chi^{\mathrm{EQ}}}{\mathrm{d}x} = -\frac{\sum_i \lambda_i(x)}{x^2}(Y_\chi^2 - (Y_\chi^{\mathrm{EQ}})^2) \tag{3.44}$$

We can now solve at $x = x_f$ using the same freeze-out criterion as before, i.e. $\Delta_\chi = cY_\chi^{\mathrm{EQ}}$ or $Y_\chi = (c+1)Y_\chi^{\mathrm{EQ}}$, to get

$$\frac{\mathrm{d}Y_\chi^{\mathrm{EQ}}}{\mathrm{d}x}(x_f) = -\frac{\sum_i \lambda_i(x_f)}{x_f^2}((c+1)^2 - 1)(Y_\chi^{\mathrm{EQ}}(x_f))^2 \quad , \tag{3.45}$$

and thus we get the general result

$$\frac{x_f^2}{Y_\chi^{\mathrm{EQ}}(x_f)} = \sum_i \lambda_i(x_f)c(c+2) \quad . \tag{3.46}$$

This dependency on $c(c+2)$ is the same for any Boltzmann equation with pairwise annihilation, balanced in equilibrium. One can now find the value of $c(c+2)$ by numerically computing the solution to the simplest form of the Boltzmann equation, and choosing c such that equation 3.36 yields the same result. This value for $c(c+2)$ then holds for any other Boltzmann equation of the form of equation 3.41, and turns out to be approximately 1.

3.1.4 An effective annihilation cross-section

The idea of an effective cross-section was introduced by B. von Harling and K. Petraki in the specific case of the formation of dark matter bound states, a process which is likely to continue after freeze-out[7]. The approach can be derived by continuing trying to solve the general Boltzmann equation 3.41. The late time limit gives us

$$\frac{\mathrm{d}Y_\chi}{\mathrm{d}x} = -\sum_i \lambda_i(x)\frac{Y_\chi^2}{x^2} \quad , \tag{3.47}$$

where the sum now only runs over annihilation channels which are no longer balanced by their respective creation channels which held the density in equilibrium in the early universe. When integrating from x_f and onward this then gives us

$$Y_\chi(\infty) = \frac{1}{\frac{1}{Y_{\mathrm{EQ}}(x_f)} + \sum_i \int_{x_i}^{\infty} \frac{\lambda_i(x)}{x^2}\mathrm{d}x} \quad , \tag{3.48}$$

Where x_f is the freeze-out time of the Dark-Matter coupled to the rest of the universe, and the x_i are the times at which the individual channels lose their balance. If the time at which a channel is no longer being compensated by creation channels is some time before freeze-out, the other processes will continue to make sure that Y_χ tracks Y_χ^{EQ}. Therefore, for those channels that have $x_i < x_f$ we use $x_i = x_f$ in the integral bounds.
For production/destruction channels that are still relevant for times after freeze-out of the Dark-Matter with the rest of the universe, such as bound-states, the integral thus starts at the specific times at which each channel becomes a one-way decay channel. A different notation for this integral would thus be

$$\int_{x_f}^{\infty} \frac{\lambda_{\mathrm{eff}}(x)}{x^2}\mathrm{d}x \quad , \tag{3.49}$$

where the effective annihilation cross-section is

$$\lambda_{\mathrm{eff}}(x) = \lambda_0(x) + \sum_i \lambda_i(x)\theta(x - x_i) \quad , \tag{3.50}$$

where λ_0 is the sum of all channels that turn into one-way channels before or at x_f. This effective method allows us to then write

$$\frac{\mathrm{d}Y_\chi}{\mathrm{d}x} = -\frac{\lambda_{\mathrm{eff}}(x)}{x^2}(Y_\chi^2 - (Y_\chi^{\mathrm{EQ}})^2) \quad , \tag{3.51}$$

where we would otherwise expect a set of coupled equations, such as with the formation of bound states. This effective Boltzmann equation will have Y_χ track Y_χ^{EQ} at times before x_f, and give an approximation to $Y_\chi(\infty)$. The only catch is that the intermediate values between x_f and ∞ could be very inaccurate, and that x_f is still defined through $\sum_i \lambda_i(x_f)$, and not $\lambda_{\text{eff}}(x_f)$. Nevertheless, when we are interested in the relic density only, it is a justified way of computing it.

3.2 Solution to the Boltzmann Equation

3.2.1 The Toy Model

As mentioned before, to model dark matter we consider a $U(1)_{\mathrm{DM}}$ gauge group, similar to QED. The minimal model that we can consider is a model with Dirac or Majorana dark matter particles, denoted as χ and $\bar{\chi}$, that can annihilate and scatter by means of a mediating boson called the Dark Photon, denoted as φ. Furthermore, if we want to consider this dark photon t be a massive particle we would also need a Dark Higgs field, or some other way of giving it its mass. The Lagrangian we can write is thus

$$\mathcal{L} = \bar{\chi}(i\not{D} - m_\chi)\chi - \frac{1}{4}F_{\mu\nu}F^{\mu\nu} \quad , \tag{3.52}$$

where $D^\mu = \partial^\mu + i\lambda A^\mu$ and $\alpha \equiv \frac{\lambda^2}{4\pi}$ is the dark mater fine structure constant.

3.2.2 Calculation of the Density Parameter

We are naturally interested in dark matter models that can reproduce the dark matter abundance observed today. The Planck results from 2015 report a Cold Dark Matter component of $\Omega_c h^2 = 0.1198$, where h is $H_0 \cdot 10^{-2}$. They also report a Hubble constant of $H_0 = 67.8$ km s^{-1} Mpc^{-1}, giving $\Omega_c = 0.261$ [8].
The density parameter is calculated as the actual density divided by the critical density, i.e. the density for which the universe is flat, such that when the total density parameter of the universe is exactly 1, the universe is flat. This effectively lets us express the different components of our universe as a fractions of the total energy content, since our universe is known to be very nearly flat. The critical density can be derived from the Friedmann equations, and is

$$\rho_{\mathrm{c}} = \frac{3H^2}{8\pi G} = \frac{3}{8\pi}H^2 m_{\mathrm{Pl}}^2 \approx 4.9 \cdot 10^{-6}\ \mathrm{GeV/cm^3} \quad , \tag{3.53}$$

making the density parameter produced by our model

$$\Omega_\chi = 2 m_\chi Y_\chi \frac{s_0}{\rho_{\mathrm{c}}} \quad , \tag{3.54}$$

where $s_0 \approx 2795/\mathrm{cm}^3$ is the entropy density of our universe and the factor of 2 accounts for the fact that we have a particle and an anti-particle, which both contribute to any observed amount of dark matter.
When numerically solving the Boltzmann equation we use $z = \frac{\alpha^2}{4}x$ as a variable and solve from $x_0 = 1$ to far beyond the point of kinetic decoupling $x_\infty \sim 100 x_{\mathrm{kd}}$. We have as an initial value to the solution $Y_\chi(z_0) = Y_\chi^{\mathrm{EQ}}(x_0)$.
The numerical solution to a Boltzmann equation with $m_\chi = 1$ TeV and $\alpha = 0.03269$ is shown in figure 3.1a. These values for the model parameters yield a present day density parameter of $\Omega_\chi = 0.26$.

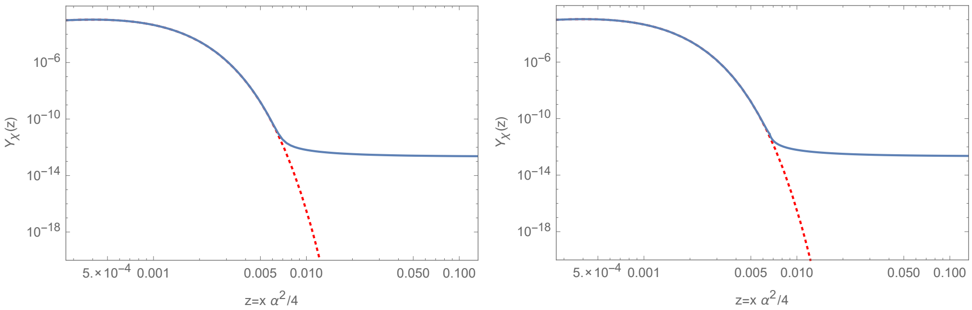

(A) Numerical solution to the Boltzmann equation.

(B) Approximate solution.

FIGURE 3.1: Plots showing (3.1a) the numerical solution, and (3.1b) the approximate solution to the Boltzmann equation 3.26, with $m_\chi = 1$ TeV and $\alpha = 0.03269$ such that $\Omega_\chi = 0.26$, accurate up to 1%. The approximate solution is a plot of equation 3.32 and 3.35. Shown in both plots is also the equilibrium distribution Y_χ^{EQ}.

We also show the analytic approach in figure 3.1b. The freeze-out time is fitted to give the right density at ∞, but even at times shortly before and after freeze-out, the approximation describes the density fairly well.

3.2.3 Newton's Method

A useful numerical tool for finding the values of our model parameters such that a relic density of $\Omega_\chi = 0.26$ is reproduced, is Newton's Method. Newton's method is a root finding algorithm used by many computational environments such as $Mathematica$. The algorithm starts with an initial guess for the root x_0, at which the tangent of the function $f(x)$ is determined. The root of the tangent of the function is then used as the next guess. The process is then repeated for the new guess until a certain precision goal is achieved.

$$x_{n+1} = x_n - \frac{f(x_n)}{f'(x_n)} \tag{3.55}$$

The algorithm can be extended to find the intersection of the function with a certain constant value F by simply finding the root of the function $(f(x) - F)$. Knowing that the constant F does not change the derivative, the algorithm is now

$$x_{n+1} = x_n - \frac{f(x_n - F)}{f'(x_n)} \quad . \tag{3.56}$$

As a termination criterion we can now use a certain percentage of F, which was previously impossible, as any percentage of 0 is 0.

When we apply this to our Boltzmann equation to find which value of α reproduces Ω_χ within 1% of 0.26 for a given value of m_χ, we obtain a straight line, as shown in figure 3.2.

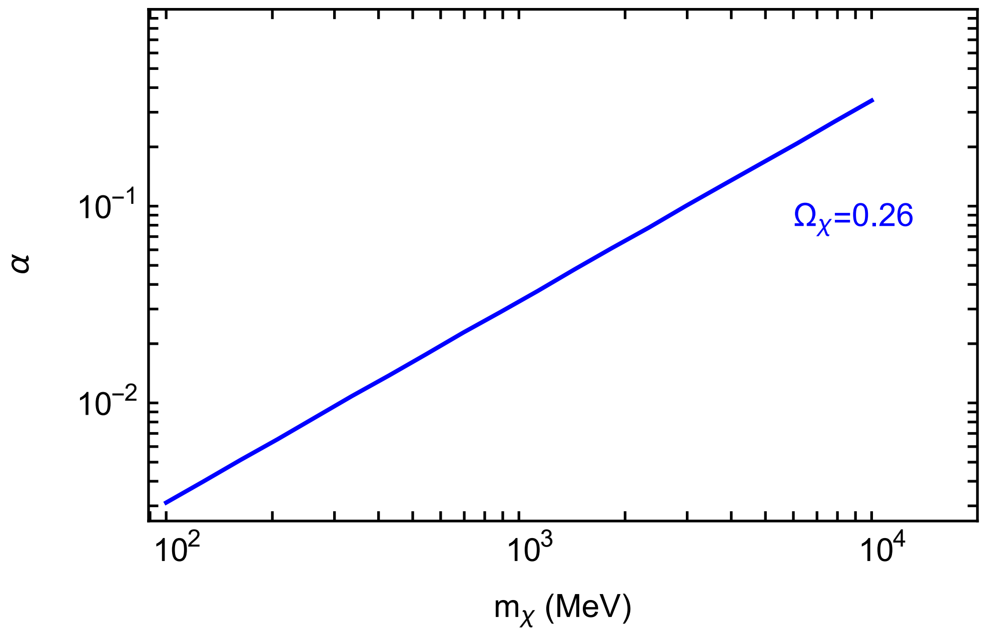

FIGURE 3.2: The relation that α and m_χ need to satisfy to produce $\Omega_\chi = 0.26$ up to 1%.

Chapter 4

Sommerfeld Enhancement of the Coulomb Potential

4.1 The Sommerfeld Enhancement

So far we have only considered a simple interaction effectively at a 4-point vertex. If the mediator in our field theory has a small mass, long range interactions might be possible, and we must consider higher order ladder diagrams.

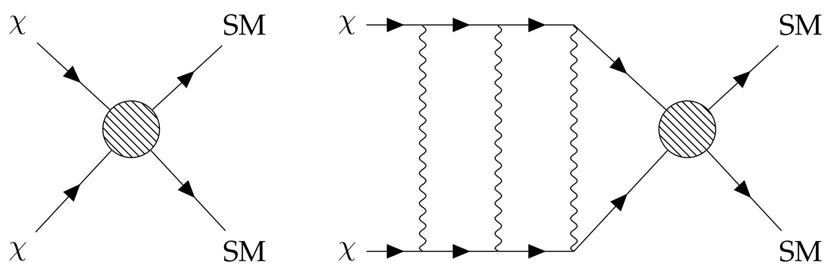

(A) Effective 4-point decay channel

(B) Ladder diagram

FIGURE 4.1: Different order annihilation diagrams. The ladder diagrams become more significant at low relative velocities and can't be treated in a perturbative fashion.[4]

For a light mediator and non-relativistic scattering particles, typically the Feynman invariant amplitude of a ladder diagram picks up a factor of α/v_{rel} per "rung". Thus, for low relative velocities, these ladder diagrams are no longer perturbative and will contribute significantly to the annihilation amplitude. To calculate the annihilation cross section properly, the diagrams must be considered up to infinite order in α/v_{rel}.
This effect, which enhances annihilation cross sections, is named the Sommerfeld Effect, after Arnold Sommerfeld, who discovered it while studying the scattering of slow moving electrons and positrons[9]. Since the most popular dark matter candidates considered are heavy, slow-moving particles, it was realized in 2003 that the effect is also relevant for calculations on dark matter annihilations[10].
When the particles are non-relativistic, it is possible to compute the Sommerfeld enhancement factor using normal quantum mechanics. The scattering amplitude is enhanced due to the probability of finding a particle at the interaction vertex being different when there is a potential. We thus have

$$\sigma_{\text{ann}} \boldsymbol{v_{\text{rel}}} = S_{\text{ann}}(v_{\text{rel}})\sigma_0 \quad \text{or} \quad S_{\text{ann}} = \frac{|\psi(0)|^2}{|\psi_0(0)|^2} \quad , \tag{4.1}$$

where ψ_0 is the wave function in absence of a potential, and $\sigma_0 \equiv (\sigma_{\text{ann}}\boldsymbol{v}_{\text{rel}})_0 = \pi\frac{\alpha^2}{m^2}$ is the first order approximation to the annihilation cross-section. We can obtain ψ by solving the time-independent Schrödinger equation for a system of two particles with momentum operators $\boldsymbol{\nabla}_1$ and $\boldsymbol{\nabla}_2$ with a potential that depends only on the relative distance. The Schrödinger equation is then

$$\left[-\frac{\boldsymbol{\nabla}_1^2}{2m_1} - \frac{\boldsymbol{\nabla}_2^2}{2m_2}\right]\psi = (E_{\text{lab}} - V(|\boldsymbol{r}_1 - \boldsymbol{r}_2|))\psi \quad . \tag{4.2}$$

This can be rewritten into relative coordinates and momenta using $\boldsymbol{\nabla}_{\text{tot}} = \boldsymbol{\nabla}_1 + \boldsymbol{\nabla}_2$ and $\boldsymbol{\nabla}_{\text{rel}}/\mu = \boldsymbol{\nabla}_1/m_1 - \boldsymbol{\nabla}_2/m_2$ as

$$\begin{aligned}\left[-\frac{\boldsymbol{\nabla}_{\text{rel}}^2}{2\mu} - \frac{\boldsymbol{\nabla}_{\text{tot}}^2}{2M}\right]\psi &= (E_{\text{lab}} - V(|\boldsymbol{r}_1 - \boldsymbol{r}_2|))\psi \\ -\frac{\boldsymbol{\nabla}_{\text{rel}}^2}{2\mu}\psi &= (E_{\text{CM}} - V(|\boldsymbol{r}_1 - \boldsymbol{r}_2|))\psi \quad ,\end{aligned}$$

where $M = m_1 + m_2$, and $\mu = m_1 m_2/M$. In the center-of-momentum frame this now describes a system of one composite particle with velocity k/μ relative to the center of momentum.

Because the potential is spherically symmetric, we can now expand ψ in terms of a radial wavefunction R_{kl} and Legendre polynomials as

$$\psi_k = \sum_l A_l R_{kl}(r) P_l(\cos\theta) \quad , \tag{4.3}$$

where the kinetic energy of the system is $E_k = \frac{k^2}{2\mu} = \frac{k^2}{m_\chi}$ for two identical particles. The azimuthal derivative then vanishes and the Schrödinger equation becomes

$$\frac{1}{r^2}\frac{\mathrm{d}}{\mathrm{d}r}r^2\frac{\mathrm{d}}{\mathrm{d}r}\psi_k + \frac{1}{r^2\sin\theta}\frac{\mathrm{d}}{\mathrm{d}\theta}\sin\theta\frac{\mathrm{d}}{\mathrm{d}\theta}\psi_k = (m_\chi V(r) - k^2)\psi_k \tag{4.4}$$

The polar angle eigenvalue of a Legendre function is easily obtained through its definition as

$$\begin{aligned}&\frac{\mathrm{d}}{\mathrm{d}x}(1-x^2)\frac{\mathrm{d}}{\mathrm{d}x}P_l(x) \equiv -l(l+1)P_l(x) \\ \Rightarrow\ &\frac{1}{\sin\theta}\frac{\mathrm{d}}{\mathrm{d}\theta}\sin\theta\frac{\mathrm{d}}{\mathrm{d}\theta}P_l(\cos\theta) = -l(l+1)P_l(\cos\theta) \quad ,\end{aligned}$$

and we thus arrive at

$$\frac{1}{r^2}\frac{\mathrm{d}}{\mathrm{d}r}r^2\frac{\mathrm{d}}{\mathrm{d}r}R_{kl} = \left[m_\chi V(r) + \frac{l(l+1)}{r^2} - k^2\right]R_{kl} \quad . \tag{4.5}$$

In absence of a potential the solutions are given by the spherical Bessel functions of order l, i.e. $R_{kl}(r) \propto j_l(kr)$. Near the origin $j_l(x) \sim x^l$, so only the $l = 0$ term is relevant in this limit. If we assume the $l = 0$ term is still the most relevant term near the origin when we have a potential, we can calculate the Sommerfeld enhancement with only the $l = 0$ partial wave considered.

Furthermore, to simplify things even more, we define $u_{kl}(r) \equiv rR_{kl}(r)$, and $u_{k0} = u_k$ to finally get

$$\frac{\mathrm{d}^2}{\mathrm{d}r^2}u_k = \left[m_\chi V(r) - k^2\right]u_k \quad . \tag{4.6}$$

For a potential that disappears at $r \to \infty$, we get as a boundary condition a plane wave solution of the form

$$u_k(\infty) = \sin(kr + \delta_V) \quad , \tag{4.7}$$

where δ_V is a phase caused by our potential. Combined with $u_k(0) = 0$ by our definition, this completely defines the boundary value problem.

4.1.1 Coulomb Potential

The general case we want to consider is the Yukawa potential,

$$V(r) = -\frac{\alpha}{r}\mathrm{e}^{-m_\phi r} \quad , \tag{4.8}$$

of which the Coulomb Potential is the special case with a massless force carrier, i.e. $m_\phi = 0$. In this case the Sommerfeld enhancement for the $l = 0$ partial wave can be computed completely analytically.
Closely following the derivation given by Steen Hannestad et al[11], the solution to the Schrödinger equation is now given by

$$\begin{aligned} \frac{\mathrm{d}^2 u_k}{\mathrm{d}x^2} &= \left[-\frac{1}{x}\mathrm{e}^{-x\frac{m_\phi}{\alpha m_\chi}} - \varepsilon^2\right] \\ &= -\frac{u_k}{x} - \varepsilon^2 u_k \quad \text{for} \quad m_\phi = 0 \quad , \end{aligned}$$

where $x = \alpha m_\chi r$ and $\varepsilon = \frac{k}{\alpha m_\chi}$. We can now solve these analytically in the limiting cases in which we know the boundary condition. For $x \to 0$ the term with ε becomes irrelevant and the general solution is given by

$$\frac{\mathrm{d}^2 u_k}{\mathrm{d}x^2} = \frac{u_k}{x} \Rightarrow u_k(x) = C_1\sqrt{x}J_1(2\sqrt{x}) + C_2\sqrt{x}Y_1(2\sqrt{x}) \quad , \tag{4.9}$$

where $J_n(x)$ and $Y_n(x)$ are the Bessel functions of the first and second kind respectively. We can expand the Bessel function into their series representations and now once more take the small x limit of our expression to get

$$\lim_{x\to 0} u_k(x) = C_1 x + \frac{C_2}{2} \quad . \tag{4.10}$$

Our boundary condition for small x then tells us that C_2 must be zero. When we look at asymptotic behavior at large x we obtain the familiar plane wave solutions.
We now take

$$u_k(x) = xv(x)\mathrm{e}^{i\varepsilon x} \quad , \tag{4.11}$$

as an Ansatz, where $v(x)$ serves to interpolate between the boundary solutions. This interpolating function is then specified through the differential equation obtained by substituting the Ansatz in the Schrödinger equation. Making the change of variable $z = -2i\varepsilon x$ yields

$$x\frac{\mathrm{d}^2 v}{\mathrm{d}x^2} + (2 + 2i\varepsilon x)\frac{\mathrm{d}v}{\mathrm{d}x} + (2i\varepsilon + 1)v = 0 \quad , \tag{4.12}$$

$$z\frac{\mathrm{d}^2 v}{\mathrm{d}z^2} + (2 - z)\frac{\mathrm{d}v}{\mathrm{d}z} - (1 - \frac{i}{2\varepsilon})v = 0 \quad . \tag{4.13}$$

4.1.2 The Confluent Hypergeometric Function ${}_1F_1(a;b;z)$

Kummer's Equation

The solution to equation 4.13 can be found by solving the more general confluent hypergeometric differential equation, also known as Kummer's equation:

$$z\frac{\mathrm{d}^2w}{\mathrm{d}z^2} + (b-z)\frac{\mathrm{d}w}{\mathrm{d}z} - aw = 0 \quad . \tag{4.14}$$

It is a second order linear differential equation, which tells us the general solution is a combination of two linearly independent solutions. We start by inferring that the solution has a power series representation of the form

$$w(z) = \sum_{n=0}^{\infty} \frac{a_n z^n}{b_n n!} \quad , \tag{4.15}$$

where the coefficients a_n and b_n are not yet determined. Substituting this expression for $w(z)$ into equation 4.14 yields

$$\sum_{n=2}^{\infty} \frac{a_n z^{n-1}}{b_n (n-1)!}(n-1) + \sum_{n=1}^{\infty} \frac{a_n z^{n-1}}{b_n (n-1)!} b - \sum_{n=1}^{\infty} \frac{a_n z^n}{b_n n!}(n) - \sum_{n=0}^{\infty} \frac{a_n z^n}{b_n n!}(a) = 0$$

$$\sum_{n=2}^{\infty} \frac{a_n z^{n-1}}{b_n (n-1)!}(b+n-1) + \left(\frac{a_n z^{n-1}}{b_n (n-1)!} b\right)\bigg|_{n=1} - \sum_{n=1}^{\infty} \frac{a_n z^n}{b_n n!}(a+n) - \left(\frac{a_n z^n}{b_n n!} a\right)\bigg|_{n=0} = 0$$

$$\sum_{n=1}^{\infty} \frac{z^n}{n!}\left[\frac{a_{n+1}}{b_{n+1}}(b+n) - \frac{a_n}{b_n}(a+n)\right] + \frac{a_1}{b_1} b - \frac{a_0}{b_0} a = 0 \quad .$$

The last expression only holds true if the coefficients of our power series satisfy the recursive relations

$$\begin{cases} a_0 = 1, \\ a_{n+1} = a_n(a+n) \end{cases} \quad \text{and} \quad \begin{cases} b_0 = 1, \\ b_{n+1} = b_n(b+n) \end{cases} \quad . \tag{4.16}$$

Thus we have our first solution, known as Kummer's solution, and commonly denoted as $M(a;b;z)$, $\Phi(a;b;z)$, or ${}_1F_1(a;b;z)$, and it is defined everywhere except for negative integer values for b.

Frobenius' method

The general approach to finding solutions using power laws, is using Frobenius' method. We assume a more general power law for $w(z)$ than the one used before, which includes the possibility of the lowest power being a real number $r \geq 0$.

$$w(z) = \sum_{n=0}^{\infty} A_n z^{n+r} \tag{4.17}$$

When substituted into equation 4.14 we get

$$\sum_{n=0}^{\infty}\left[\frac{n+r}{z}(r+b+n-1)-(a+n+r)\right]A_n z^{n+r}=0$$
$$r(r-1+b)A_0 z^{r-1}+((r+1)(r+b)A_1-(r+a)A_0)z^r+O(z^{r+1})=0 \quad .$$

Since this must hold for any value of z, we get that in the limit of $z\to 0$ all $O(z^{r+1})$ terms vanish, and are left with

$$\lim_{z\to 0}\left[r(r-1+b)A_0 z^{r-1}+((r+1)(r+b)A_1-(r+a)A_0)z^r\right]=I(r)=0 \quad , \tag{4.18}$$

which is known as the Indical equation, or the Indical polynomial. In this limit the first term is singular. However, there are two values of r for which this term cancels. For $r=0$ we obtain the result we derived before, and find the value for A_0. The other value for the lowest possible power is $r=1-b$.
When we now substitute $w(z)=z^{1-b}v(z)$ into equation 4.14, we find an equation for v that can be solved using $v(z)=M(a+1-b;2-b;z)$, giving $w(z)=z^{1-b}M(a+1-b;2-b;z)$.
The two solutions we now have for w can be used in linearly independent functions which solve Kummer's equation in most of parameter space. However, because of the nature of coefficients a_n and b_n, the solutions break down or can even become equal. At points in parameter space where either or both of these solutions break down, different solution methods exist to still provide the two solutions that make up a general solution to the problem. These methods depend very specifically on the parameters in question, but they are, however, always based around Kummer's original solution, $M(a;b;z)$.

Asymptotic limit of M(a;b;z)

We now have $M(1-\frac{i}{2\varepsilon};2;-2i\varepsilon x)$ as a candidate for one of the solutions for $v(x)$ in equation 4.13. Assuming it doesn't break down for the given parameters $\{a,b\}$, we thus have a general solution of the form

$$v(x)=C_1 M(1-\frac{i}{2\varepsilon};2;-2i\varepsilon x)+C_2 f(a;b;z) \quad , \tag{4.19}$$

where $f(z)$ is the other solution.

The asymptotic form of $M(a;b;|z|\mathrm{e}^{i\varphi})$ for $|z|\to\infty$, with $\varphi=-\frac{\pi}{2}$ is [12]

$$\lim_{|z|\to\infty} M(a;b;z)=\frac{\Gamma(b)}{\Gamma(a)}\mathrm{e}^z z^{a-b}+\frac{\Gamma(b)}{\Gamma(b-a)}\mathrm{e}^{-i\pi a}z^{-a} \quad . \tag{4.20}$$

In our case we have $b-a=a^*$, and thus we can write $\Gamma(a)=|\Gamma(a)|\mathrm{e}^{i\eta}$ and $\Gamma(b-a)=|\Gamma(a)|e^{-i\eta}$. We get for $a=1-\frac{i}{2\varepsilon}$ and $b=2$ that

$$\lim_{x\to\infty} M(1-\frac{i}{2\varepsilon};2;-2i\varepsilon x)=\frac{\mathrm{e}^{-\frac{\pi}{4\varepsilon}}\mathrm{e}^{-i\varepsilon x+i\eta}}{\Gamma(1-\frac{i}{2\varepsilon})\varepsilon x}\sin(\varepsilon x+\eta+\frac{1}{2\varepsilon}\ln(2\varepsilon x)) \quad . \tag{4.21}$$

This means that if we choose C_1 to be

$$C_1=\frac{\varepsilon\Gamma(1-\frac{i}{2\varepsilon})}{\mathrm{e}^{-\frac{\pi}{4\varepsilon}}\mathrm{e}^{i\eta}} \quad , \tag{4.22}$$

our boundary value problem is satisfied completely by our Ansatz with just $M(a;b;z)$ as a solution. We can therefore set $C_2 = 0$ without having to worry about what the second solution even is.

We can now calculate the probability of finding the reduced mass particle at the origin to be

$$|\psi(0)|^2 = \frac{|\Gamma(1+\frac{i}{2\varepsilon})|^2}{\mathrm{e}^{-\frac{\pi}{2\varepsilon}}}|k|^2 \quad . \tag{4.23}$$

This also gives us $|\psi_0(0)| = |k|^2$, since the potential vanishes when α is set to zero, or equivalently, $\varepsilon \to \infty$.
Furthermore, Euler's reflection formula tells us that

$$\Gamma(1-z)\Gamma(z) = \frac{\pi}{\sin(\pi z)} \quad , \tag{4.24}$$

which we can rewrite using the definition of the Gamma function, $\Gamma(1+z) = z\Gamma(z)$, to get

$$\Gamma(1-z)\Gamma(1+z) = \frac{\pi z}{\sin(\pi z)} \tag{4.25}$$

$$\Rightarrow |\Gamma(1+i\gamma)|^2 = \frac{\pi\gamma}{\sinh(\pi\gamma)} \quad . \tag{4.26}$$

We then finally arrive at

$$\begin{aligned} S_{\text{ann}} = \frac{|\psi(0)|^2}{|\psi_0(0)|^2} &= \frac{\frac{\pi}{\varepsilon}}{1-\mathrm{e}^{-\frac{\pi}{\varepsilon}}} \\ &= \frac{2\pi\zeta}{1-\mathrm{e}^{-2\pi\zeta}} \quad , \end{aligned}$$

where we have defined $\zeta \equiv \frac{\alpha}{v} = \alpha\frac{\mu}{k} = \frac{1}{2\varepsilon}$ out of convention.

4.1.3 Thermally Averaged Cross-section

We would now like to write the cross-section as a function of time, or the temperature of the universe, rather than the velocities of individual particles, which may have arbitrary values from a certain distribution at any given instant. This process is known as thermal averaging, and it is done by summing the cross-section over all velocities, weighing each velocity by its probability[5].

$$\langle\sigma_{\text{ann}}|\boldsymbol{v}_{\text{rel}}|\rangle \equiv \int (\sigma_{\text{ann}}|\boldsymbol{v}_{\text{rel}}|) f(\boldsymbol{v}_1) f(\boldsymbol{v}_2) \mathrm{d}^3\boldsymbol{v}_1 \mathrm{d}^3\boldsymbol{v}_2 \tag{4.27}$$

Here, σ_{ann} and $\boldsymbol{v}_{\text{rel}} = \boldsymbol{v}_1 - \boldsymbol{v}_2$ are functions of just the relative velocity, so we can rewrite the integral into an integral over $\boldsymbol{v}_{\text{rel}}$ and $\boldsymbol{v}_{\text{tot}}$, with a Jacobian of $\frac{1}{8}$. When we take a Maxwell-Boltzmann velocity distribution, i.e.

$$f(\boldsymbol{v}) = \left(\frac{x}{2\pi}\right) \mathrm{e}^{-\frac{x}{2}|\boldsymbol{v}|^2} \quad , \tag{4.28}$$

where $x = \frac{m}{T}$, the integral over $\boldsymbol{v}_{\text{tot}}$ is then just a Gaussian integral, and we are left with

$$\frac{x^{\frac{3}{2}}}{2\sqrt{\pi}} \int (\sigma_{\text{ann}}|\boldsymbol{v}_{\text{rel}}|)|\boldsymbol{v}_{\text{rel}}|^2 \mathrm{e}^{-\frac{x}{4}|\boldsymbol{v}_{\text{rel}}|^2} |\boldsymbol{v}_{\text{rel}}|^2 \mathrm{d}|\boldsymbol{v}_{\text{rel}}| \quad . \tag{4.29}$$

Because we have defined $\sigma_{\text{ann}} \equiv S_{\text{ann}}\sigma_0$, and $\sigma_0 = \frac{\alpha^2}{m^2}$, we get

$$\langle \sigma_{\text{ann}} |\boldsymbol{v}_{\text{rel}}| \rangle = \sigma_0 \bar{S}_{\text{ann}} \quad , \tag{4.30}$$

where

$$\bar{S}_{\text{ann}}(x) = \frac{x^{\frac{3}{2}}}{2\sqrt{\pi}} \int_0^\infty S_{\text{ann}}(\alpha/\boldsymbol{v}_{\text{rel}}|)|\boldsymbol{v}_{\text{rel}}|^2 \mathrm{e}^{-\frac{x}{4}|\boldsymbol{v}_{\text{rel}}|^2} \mathrm{d}|\boldsymbol{v}_{\text{rel}}|$$
$$\bar{S}_{\text{ann}}(z) = \frac{2}{\sqrt{\pi}} \int_0^\infty S_{\text{ann}}(\sqrt{z/u})\sqrt{u}\mathrm{e}^{-u}\mathrm{d}u \quad ,$$

is the thermally averaged cross-section expressed in terms of $z = \frac{\alpha^2}{4}x$.

4.1.4 Relic Density with a Coulomb potential

If we consider dark matter particles which can interact and annihilate through a massless mediator, after taking the Sommerfeld effect into account we obtain

$$\frac{\mathrm{d}Y_\chi}{\mathrm{d}z} = -\frac{\lambda_1 \bar{S}_{\text{ann}}(z)}{z^2}(Y_\chi^2 - (Y_\chi^{\text{EQ}})^2) \quad , \tag{4.31}$$

where

$$\lambda_1 = \sqrt{\frac{\pi}{45}} m_{\text{Pl}} m_\chi \frac{\alpha^2}{4} \sigma_0 \frac{g_*^{(p)}}{\sqrt{g_*^{(\rho)}}} \quad . \tag{4.32}$$

To reproduce the present day density parameter of $\Omega_\chi = 0.26$, we again use Newton's method to find a value for α for each value of m_χ. The results, together with the results from the previous chapter are shown in figure 4.2a.

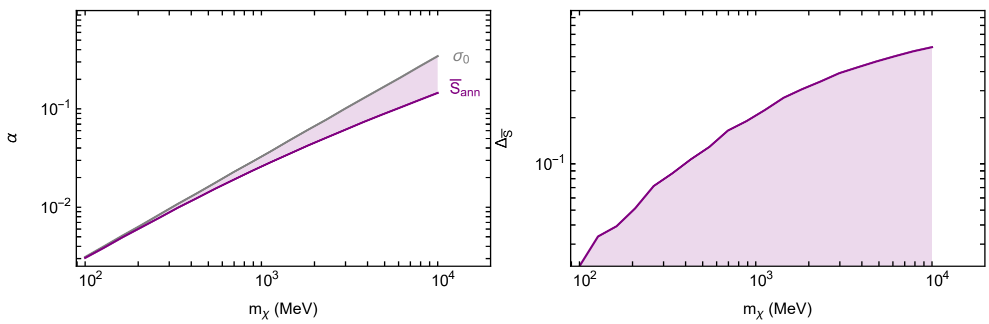

(A) (B)

FIGURE 4.2: (4.2a) The numerical results of solving the Sommerfeld Enhanced Boltzmann equation. The enhanced annihilation cross-section for increasing m_χ consequently requires α to be smaller in order for the solution to yield $\Omega_\chi = 0.26$. The previously obtained numerical results for the 4-point annihilation case are also shown. (4.2b) Relative difference between the σ_0 and the Sommerfeld enhanced case.

We have also shown the relative difference $\Delta_{\bar{S}}$ between the new results and those from previous chapter. It is calculated as the absolute difference between the two results divided by the results for the non-enhanced case.

$$\Delta_{\bar{S}} = \frac{|\alpha_{\sigma_0} - \alpha_{\bar{S}}|}{\alpha_{\sigma_0}} \tag{4.33}$$

For larger values of m_χ the Sommerfeld enhancement can reach values of over 50%, proving that it is very significant, and that it must be accounted for in any relic density calculation.

4.2 Dark Matter Bound State Formation

The possibility of the dark matter forming bound states becomes more important at low relative velocities. Two dark matter particles can, under emission of a dark photon, form a bound state. The bound state can similarly ionize back into dark matter by absorbing a dark photon, or it can decay into dark photons. The bound states can be treated analogous to positronium bound states, i.e. states made of an electron-positron pair[1]. The binding energy of a bound state can be calculated to be $E_n = \frac{\mu\alpha^2}{2n^2}$. We differentiate between para-darkonium, a spin 0 singlet, and ortho-darkonium, a spin 1 triplet. It can be shown, due to the anti-symmetry in the wave-functions, that the singlet can only decay into an even number of photons (≥ 2 due to momentum conservation), while the triplet decays into an odd number of photons (≥ 2).

4.2.1 The Sommerfeld Enhancement for Bound States

[13] Just like with the Sommerfeld enhancement for annihilation we can write

$$\sigma^{(n)}_{\mathrm{BSF}} v_{\mathrm{rel}} = \sigma_0 S^{(n)}_{\mathrm{BSF}}(\zeta) \quad . \tag{4.34}$$

The sommerfeld Enhancement for the n-th level is

$$S^{(n)}_{\mathrm{BSF}}(\zeta) = (1/n) S^{(1)}_{\mathrm{BSF}}(\zeta/n) \quad , \tag{4.35}$$

where

$$S^{(1)}_{\mathrm{BSF}}(\zeta) = S_{\mathrm{ann}}(\zeta)\frac{2^9}{3}\frac{\zeta^4}{(1+\zeta^2)^2}\mathrm{e}^{-4\zeta \mathrm{arccot}\zeta} \quad . \tag{4.36}$$

The total cross section is the sum over all energy levels,

$$S^{\mathrm{tot}}_{\mathrm{BSF}}(\zeta) = \sum_{n=1}^{\infty} S^{(n)}_{\mathrm{BSF}}(\zeta) \tag{4.37}$$

For large ζ, or low relative velocities, the expression for $S^{(1)}_{\mathrm{BSF}}$ simplifies, and the total enhancement factor then becomes

$$\lim_{\zeta \gg 1} S^{\mathrm{tot}}_{\mathrm{BSF}}(\zeta) = \frac{\pi^2}{6} S^{(1)}_{\mathrm{BSF}}(\zeta) \quad . \tag{4.38}$$

From this it becomes evident that even when the relative velocity is very low, the ground state still contributes the most to the enhancement.
The thermal averaged Sommerfeld enhancement is weighed by an extra factor of $(1 + f(E_n + \mu|\boldsymbol{v}_{\mathrm{rel}}|^2/2))$, due to the dark photon Bose-enhancing the formation process. This enhancement is particularly significant because it helps establish a bound state

[1] Dark Matter bound states are therefore sometimes suggestively called Darkonium to complete the analogy.

concentration as the universe leaves equilibrium.

$$\bar{S}_{\text{BSF}}(z_\chi, z_\varphi) = \frac{2}{\sqrt{\pi}} \int_0^\infty S_{\text{BSF}}\left(\sqrt{z_\chi/u}\right) \frac{\sqrt{u}\mathrm{e}^{z_\varphi}}{\mathrm{e}^{z_\varphi - u} - 1} \mathrm{d}u \tag{4.39}$$

Generally, the dark matter has the same temperature as the rest of the universe, which is relayed through the dark photon background. We can therefore take z_χ and z_φ to be equal[2].

4.2.2 Ionization and Decay of Bound States

The decay rates for para-positronium and ortho-positronium respectively are[14]

$$\Gamma_{\uparrow\downarrow} = \mu\alpha^5 \quad \text{and} \quad \Gamma_{\uparrow\uparrow} = \mu\alpha^5\lambda_\alpha \quad , \tag{4.40}$$

where $\lambda_\alpha = 4\alpha(\frac{\pi}{9} - \frac{1}{\pi})$. The ionization cross-section can be derived using the Milne relation and the cross-section for the formation process:

$$\frac{\sigma_{\text{ion}}(\omega)}{\sigma_{\text{BSF}}(|\boldsymbol{v}_{\text{rel}}|)} = \frac{2\omega^2}{\mu^2|\boldsymbol{v}_{\text{rel}}|^2} \quad . \tag{4.41}$$

$$\Gamma_{\text{ion}}(z) = \frac{3}{2\pi^2}\int_\Delta^\infty f_\varphi(\omega)\sigma_{\text{ion}}\omega^2 \mathrm{d}\omega = \mu\alpha^5 f_{\text{ion}}(z) \quad ,$$
$$f_{\text{ion}}(z) \equiv \frac{2^7}{3}\int_0^\infty \frac{\eta}{(1+\eta^2)^2} \frac{\mathrm{e}^{-4\eta \operatorname{arccot}\eta}}{1-\mathrm{e}^{-2\pi\eta}} \frac{1}{\mathrm{e}^{z(1+1/\eta^2)} - 1}\mathrm{d}\eta \quad .$$

4.2.3 Coupled Boltzmann equations

Rather than writing down a single Boltzmann equation describing the density of dark matter, balanced by an equilibrium distribution, we can also write a set of coupled equations to keep track of our exact bound state density. We get[7]

$$\begin{aligned}
\frac{\mathrm{d}Y_\chi}{\mathrm{d}z} &= -\frac{\lambda_1 \bar{S}_{\text{ann}}(z)}{z^2}(Y_\chi^2 - Y_\chi^{\text{EQ}}(\frac{4}{\alpha^2}z)^2) - \frac{\lambda_1 \bar{S}_{\text{BSF}}(z)}{z^2} + \lambda_2 z f_{\text{ion}}(z)(Y_{\uparrow\downarrow} + Y_{\uparrow\uparrow}) \quad , \\
\frac{\mathrm{d}Y_{\uparrow\downarrow}}{\mathrm{d}z} &= \frac{\lambda_1 \bar{S}_{\text{BSF}}(z)}{4z^2}Y_\chi^2 - \lambda_2 z(1 + f_{\text{ion}}(z))Y_{\uparrow\downarrow} \quad , \\
\frac{\mathrm{d}Y_{\uparrow\uparrow}}{\mathrm{d}z} &= \frac{3\lambda_1 \bar{S}_{\text{BSF}}(z)}{4z^2}Y_\chi^2 - \lambda_2 z(\lambda_\alpha + f_{\text{ion}}(z))Y_{\uparrow\uparrow} \quad ,
\end{aligned}$$

where

$$\lambda_2 = 4\sqrt{\frac{45}{\pi^3 g_*^{(\rho)}}\frac{m_{\text{Pl}}}{m_\chi}}\alpha \quad . \tag{4.42}$$

As initial conditions we use

$$\begin{aligned}
&Y_\chi(z_0) = Y_\chi^{\text{EQ}}(x_0) \quad , \\
&Y_{\uparrow\downarrow}(z_0) = \frac{1}{g_\chi}Y_\chi^{\text{EQ}}(2x_0 - z_0) \quad \text{and} \quad Y_{\uparrow\uparrow}(z_0) = 3Y_{\uparrow\downarrow}(z_0) \quad .
\end{aligned}$$

[2]Note that $z_\varphi = m_\chi/T_\varphi$, still normalized by m_χ, and not m_ϕ.

For the bound state we have $E/T = (2m_\chi - \frac{m_\chi \alpha}{4})/T = 2x - z$. For non-relativistic particles ($E = m$) this shows how the mass of bound states is effectively the mass of their constituents minus the binding energy.
The results are shown in figure 4.3. The formation of bound states lowers the necessary α even further, compared to just the Sommerfeld enhancement.

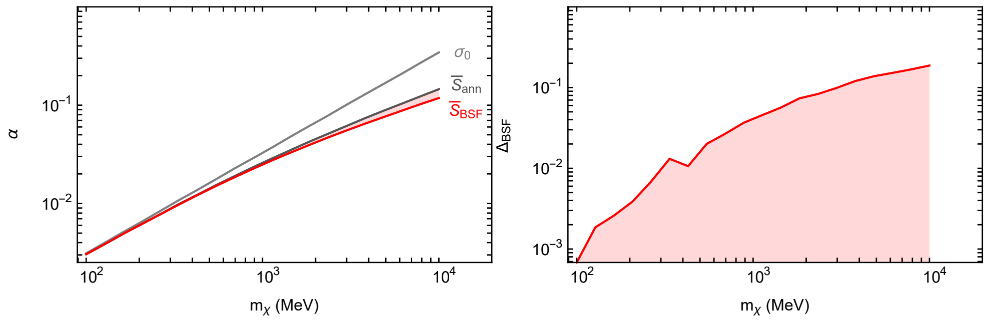

FIGURE 4.3: The numerical results for solving the coupled Boltzmann equations with bound-state formation considered. The previously obtained results are also shown.

The relative difference with the Smmerfeld enhanced case, i.e.

$$\Delta_{\rm BSF} = \frac{|\alpha_{\bar{S}_{\rm ann}} - \alpha_{\bar{S}_{\rm BSF}}|}{\alpha_{\bar{S}_{\rm ann}}} \quad , \tag{4.43}$$

reaches values over 10%, making the formation of bound states a significant enough process to account for when considering non-relativistic dark matter.

4.3 Effective Approach

As previously discussed, when we are interested in only the relic density, we can take the late time limit of our Boltzmann equation and find that we only need to solve one equation rather than three. The density after freeze-out only depends on which annihilation channels are effectively only one-way processes. We have

$$Y_\chi(\infty) = \frac{1}{\frac{1}{Y_\chi^{\rm EQ}(x_f)} + \int_{z_f}^{z_{\rm kd}} \frac{\lambda_{\rm eff}(z)}{z^2} {\rm d}z} \quad , \tag{4.44}$$

where x_f is determined by solving

$$x_f - \frac{1}{2}\ln(x_f) - \ln(\bar{S}_{\rm ann}(z_f) + \bar{S}_{\rm BSF}(z_f)) = \ln\left(\frac{3\sqrt{\frac{5}{2}}}{4\pi^2}\frac{g_\chi}{\sqrt{g_*^{(\rho)}}} m_{\rm Pl}\frac{\alpha^2}{m_\chi}\right) \quad , \tag{4.45}$$

and $z_f = \frac{\alpha^2}{4} x_f$. For bound-states we have

$$\lambda_{\rm eff}(z) = \lambda_1 \times \begin{cases} \bar{S}_{\rm ann} & z_f < z < f_{\rm ion}^{-1}(1) \approx 0.28 \\ \bar{S}_{\rm ann} + \frac{\bar{S}_{\rm BSF}}{4} & 0.28 < z < f_{\rm ion}^{-1}(\lambda_\alpha) \\ \bar{S}_{\rm ann} + \bar{S}_{\rm BSF} & f_{\rm ion}^{-1}(\lambda_\alpha) < z \end{cases} \quad , \tag{4.46}$$

where the bounds of the different intervals are determined by the values of z for which the decay rate of the para-(ortho-)darkonium $\Gamma_{\uparrow\downarrow}(\Gamma_{\uparrow\uparrow})$ dominates over the ionization rate Γ_{ion}. The balance between f_{ion} and the decay coefficients thus govern whether bound state formation channels effectively act as one-way channels or not. If the probability of ionization becomes significantly less that the probability of decay, we can treat the dark matter particles that form bound states as if they have annihilated already.

The results of computations using this effective method match the numerical results very well. Figure 4.4 shows the results of the effective method relative to numerical results, for all three scenarios discussed so far. Note how the σ_0 and Sommerfeld enhanced cases are actually just the analytical approximation to the Boltzmann equation. Only the bound state case makes actual use of effective annihilation cross-sections. Nevertheless the accuracy of all three cases appears to be mostly of the same order. Thus the effective method is a good generalization of the analytical approximation used for a single Boltzmann equation. Moreover the accuracy of the effective method does not reach values higher than 2.5%, making it a useful tool to study the effects where difficult computations are involved, especially when these processes affect the values of α by more than 10%.

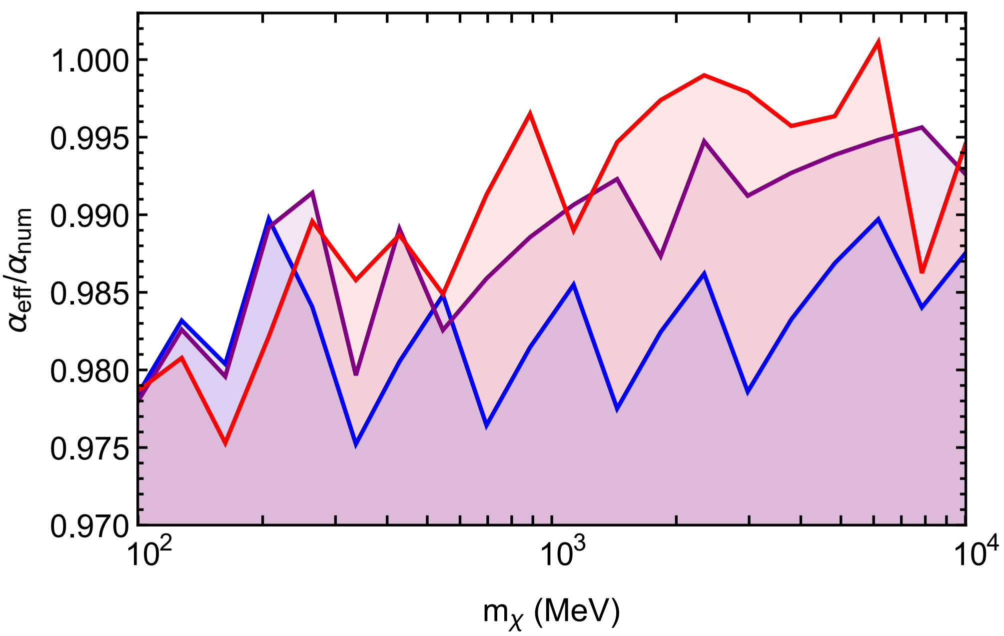

FIGURE 4.4: Results for using the effective method relative to numerical results. Shown are the three cases studied before, with the σ_0 case being the blue graph, $\bar{S}_{\text{ann}}$ being the purple one, and $\bar{S}_{\text{BSF}}$ being the red. The results using the effective method don't deviate more then 2.5% from numerical results.

Chapter 5

Sommerfeld Enhancement with a Massive Mediator

It is not unthinkable that dark matter could be mediated by a massive force-carrier. In fact, neutrinos constitute a form of dark matter, although their contribution is small, and they interact with leptons using the weak force gauge bosons, which are all massive. Weakly Interacting Massive Particles (WIMPs) are also a renowned candidate for dark matter. Supersymmetry (SUSY) predicts particles that interact through the electroweak force with a typical cross section and mass that very closely gives the right dark matter abundance. Neutralinos, the heavier superpartners of neutrinos, are a good candidate for dark matter predicted by SUSY.
When considering a toy model it would be relatively unfruitful to not generalize to a massive mediator.

5.1 The Yukawa Potential

When we add mass to the propagator of our mediator particle, we obtain the Yukawa potential, as defined earlier in chapter 4.

$$V(\boldsymbol{r}) = -\frac{\lambda^2}{(2\pi)^3}\int \mathrm{e}^{-i\boldsymbol{k}\cdot\boldsymbol{r}}\frac{4\pi}{\boldsymbol{k}^2+m^2}\mathrm{d}^3\boldsymbol{k} = -\frac{\lambda^2}{r}\mathrm{e}^{-m_\varphi r} \tag{5.1}$$

There are many ways to treat the Yukawa potential, aside from solving the Schrödinger equation numerically. The Yukawa potential can, for example, be approximated by the Hulthén potential,

$$V_Y(r) \approx V_{\mathrm{H}}(r) = \frac{\pi^2}{6}\frac{\alpha m_\varphi}{\mathrm{e}^{\frac{\pi^2}{6}m_\varphi r}-1} \quad . \tag{5.2}$$

For $l = 0$ this approximation is very good, but for $l \neq 0$ a better approximation includes a centrifugal term[15].

$$\tilde{V}_l(r) = \frac{l(l+1)}{m_\chi}\left(\frac{\pi^2 m_\varphi}{6}\right)^2\frac{\mathrm{e}^{-\frac{\pi^2}{6}m_\varphi r}}{(1-\mathrm{e}^{-\frac{\pi^2}{6}m_\varphi r})^2} \tag{5.3}$$

It is then possible to analytically calculate the approximate Sommerfeld enhancement for the Yukawa potential[16]. For the $l = 0$ case, the result is

$$S_Y(\zeta,\xi) \approx S_H(\zeta,\xi) = \left| \frac{\Gamma(1 + i\frac{\xi}{2\zeta}(1 - \sqrt{1 - \frac{4\zeta^2}{\xi}}))\Gamma(1 + i\frac{\xi}{2\zeta}(1 + \sqrt{1 - \frac{4\zeta^2}{\xi}})}{\Gamma(1 + i\frac{\xi}{\zeta})} \right|^2 . \tag{5.4}$$

Using Eulers reflection formula, equation 4.26, we can simplify this into

$$S_{l=0}(\zeta,\xi) = \frac{2\pi\zeta \sinh(\pi\frac{\xi}{\zeta})}{\cosh(\pi\frac{\xi}{\zeta}) - \cosh(\pi\frac{\xi}{\zeta}\sqrt{1 - \frac{2\zeta^2}{\xi}})} \quad , \tag{5.5}$$

where $\zeta = \frac{\alpha}{v}$ and $\xi = \frac{\alpha m_\chi}{2m_\varphi}$. The approximation using the Hulthén potential and the results of solving the Schrödinger equation with the exact Yukawa potential are shown in figure 5.1.

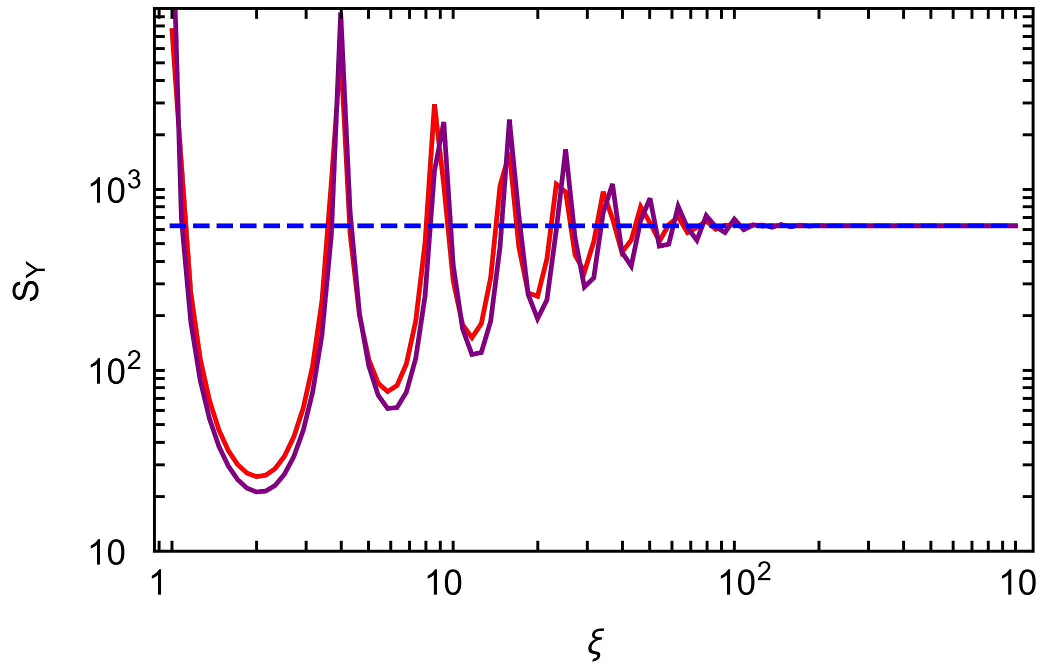

FIGURE 5.1: Plot of the numerical results of solving the Schrödiner equation with the Yukawa potential and the approximation obtained for the Hulthén potential. Also shown is the Coulomb limit ($\xi \to \infty$), which is approached by both the numerical result and the approximation.

After performing the thermal averaging integral of the Sommerfeld enhancement for both the numerically solved Schrödinger equation with the exact Yukawa potential and the Sommerfeld enhancement for the Huelthen potential, we find that the percentual difference between the two is around 10^{-3} for most values of z. The difference does not rise above 10^{-3} for $z > z_f$, which is the domain we integrate over when using the effective method to calculate the relic density. The values of α, m_χ, and m_φ that lead to a density parameter of $\Omega_\chi = 0.26$ are shown in figure 5.2.

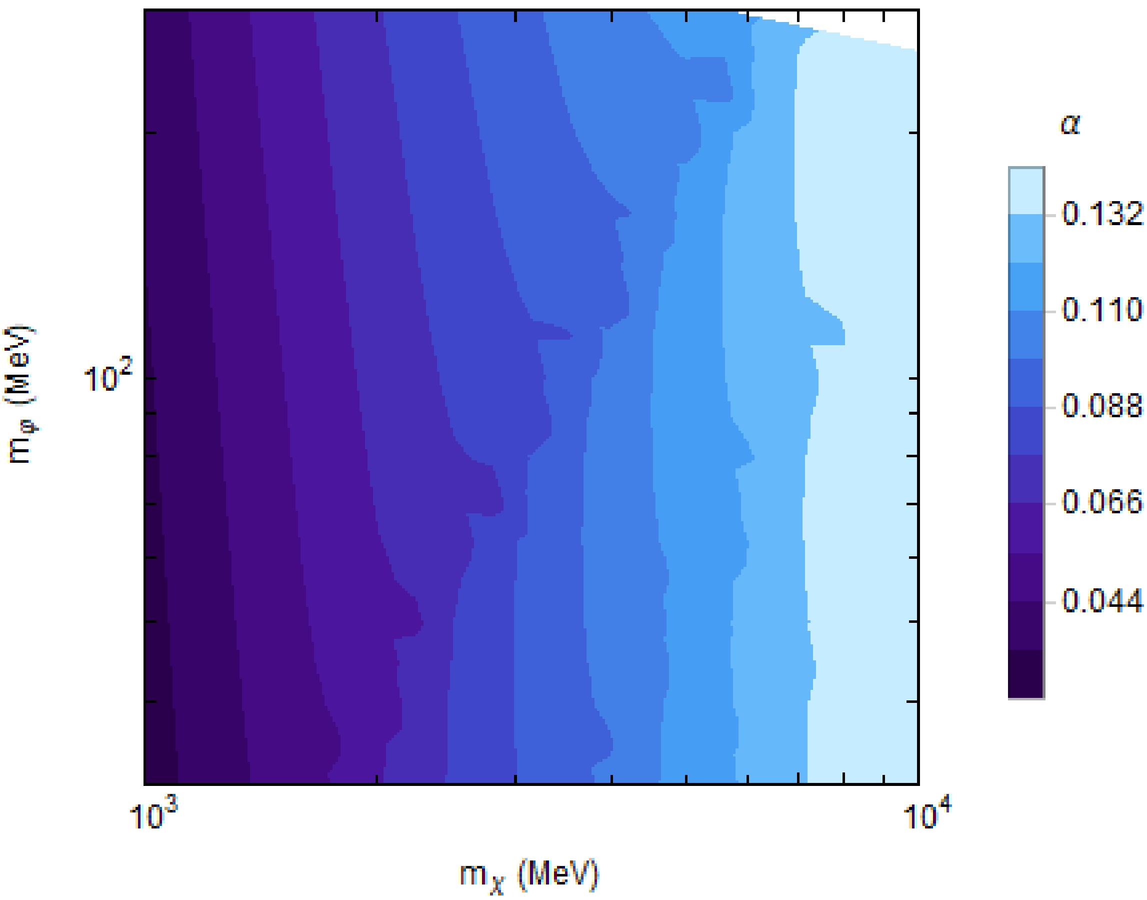

FIGURE 5.2: Logarithmic contour plot of α calculated for various values of m_χ and m_φ using the effective method. Slightly visible are two streaks of resonances where α is suddenly lower than for the surrounding points in parameter space. The values for α were calculated for 21 values of m_χ ranging from 10^3 GeV to 10^4 GeV. The values of m_φ range from $10\sqrt{10}$ GeV to $10^{2.45}$ GeV in 20 steps. The white spots are where *Mathematica* returned nonsensical values.

As with the $m_\varphi = 0$ case, we see that α increases with m_χ. Moreover, we also have resonances at certain values of m_χ and m_φ, such that the thermally averaged annihilation cross-section is much higher, and we therefore need a slightly lower value for α. It might be noteworthy that because of these resonances, for a fixed value of m_χ and α there are multiple values that m_φ can take that result in the same Ω.

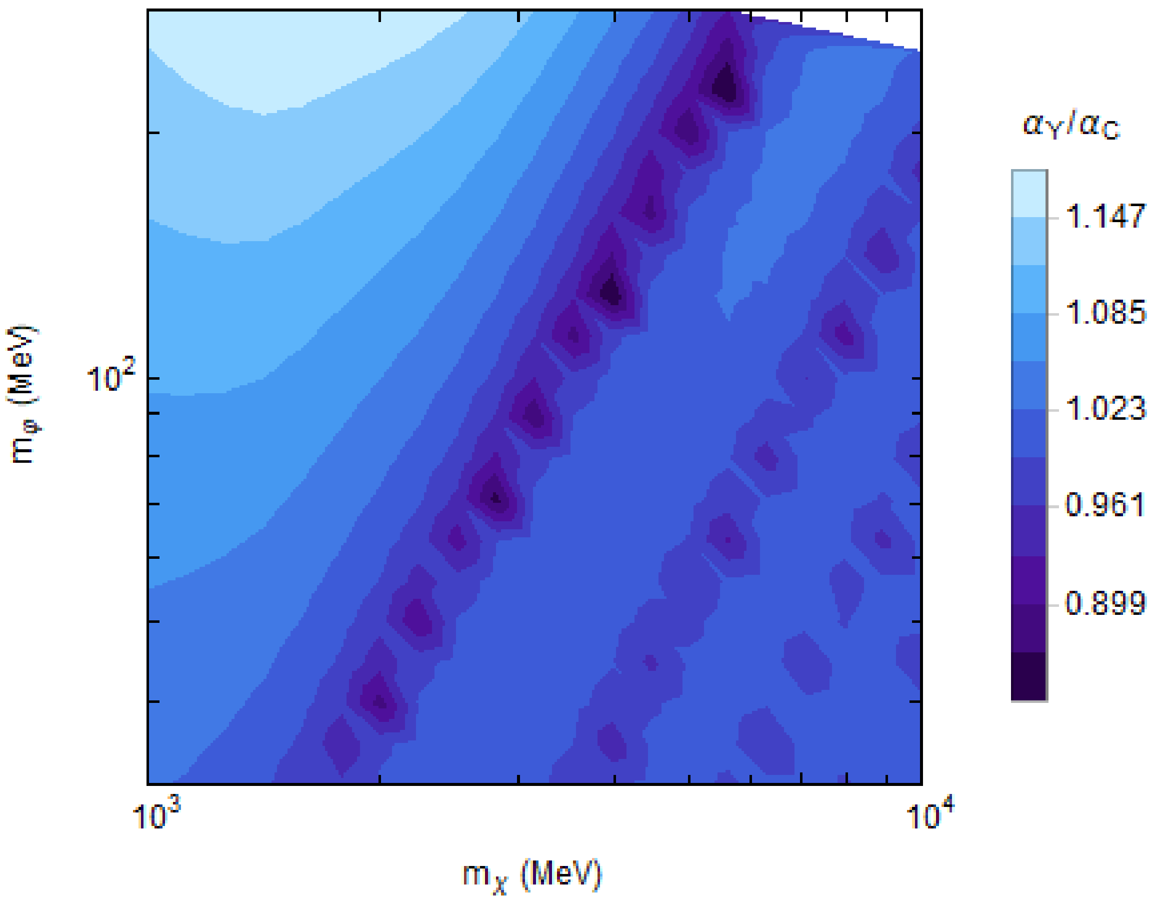

FIGURE 5.3: Results for the Yukawa potential relative to the Coulomb ($m\varphi = 0$) case. The resonances are made more clear.

Figure 5.3 shows the further enhancement a massive mediator can provide, relative to the massless case. The resonances are very clear this way, and they lie on lines where roughly $m_\varphi \sim m_\chi^2$. At these resonances α can be further reduced by as much as $\sim 15\%$.

Chapter 6

Conclusion

A theoretical model of symmetric cold dark matter can, using the Boltzmann equation, predict a present day relic density parameter Ω_χ which is highly dependent on the thermally averaged cross-section $\langle\sigma|v_{\text{rel}}|\rangle$ of the involved processes. For specific values of m_χ and α the real world value of $\Omega_c = 0.26$ can be matched. When the mediating dark photon mass m_φ is small or zero, the effect known as the Sommerfeld enhancement can significantly enhance the cross-section. For high values of m_χ (> 10 TeV) the corresponding value for α can be a factor of 2 less than the non-enhanced case would predict.
In scenarios where the Sommerfeld enhancement is relevant, the formation of bound states could also have a significant impact on the values that the parameters of the model can take. For large m_χ (> 10 TeV) the value of α can be reduced by another 20%.
In the case where our dark photon is a massive mediator, for certain values of m_χ and m_φ the enhancement factor can have resonance peaks. At these peaks the value for α can come to lie another 15% lower compared to the massless case, making the Sommerfeld enhancement relevant at lower values of m_χ too.
In future calculations on thermal relic dark matter models all these effects should be taking into account. The formation of bound states should also be investigated in the case of a Yukawa interaction to see if this also affects the values of the allowed model parameters significantly.

Bibliography

[1] F. Zwicky. “Die Rotverschiebung von extragalaktischen Nebeln”. In: *Helvetica Physica Acta* 6 (1933), pp. 110–127. URL: http://adsabs.harvard.edu/abs/1933AcHPh...6..110Z.

[2] F. Zwicky. “On the Masses of Nebulae and of Clusters of Nebulae”. In: *The Astophysical Journal* 86 (Oct. 1937), p. 217. DOI: 10.1086/143864.

[3] V. C. Rubin, W. K. Ford Jr., and N. Thonnard. “Rotational properties of 21 SC galaxies with a large range of luminosities and radii, from NGC 4605 /R = 4kpc/ to UGC 2885 /R = 122 kpc/”. In: *The Astophysical Journal* 238 (June 1980), pp. 471–487. DOI: 10.1086/158003.

[4] Joshua Ellis. “TikZ-Feynman: Feynman diagrams with TikZ”. In: (2016). arXiv: 1601.05437.

[5] Jonathan L. Feng, Manoj Kaplinghat, and Hai-Bo Yu. “Sommerfeld enhancements for thermal relic dark matter”. In: *Phys. Rev.* 82 (2010). arXiv: 1005.4678v3.

[6] E. W. Kolb and M. S. Turner. *The Early Universe*. Westview Press, 1994.

[7] Benedict von Harling and Kalliopi Petraki. “Bound-state formation for thermal relic dark and unitarity”. In: (2014). arXiv: 1407.7874v2.

[8] P. A. R. Ade et al. “Planck 2015 results XIII. Cosmological parameters”. In: (2015). arXiv: 1502.01589v3.

[9] A. Sommerfeld. “Über die Beugung und Bremsung der Elektronen”. In: *Ann.Phys* 403 (Mar. 1931), 257–330. DOI: 10.1002/andp.19314030302.

[10] J. Hisano, S. Matsumoto, and M. M. Nojiri. “Unitarity and higher order corrections in neutralino dark matter annihilation into two photons”. In: *Phys.Rev.* (June 2003), pp. 471–487. DOI: 10.1103/PhysRevD.67.075014.

[11] Steen Hannestad and Thomas Tram. “Sommerfeld Enhancement of DM Annihilation: Resonance Structure, Freeze-Out and CMB Spectral Bound”. In: (2011). arXiv: 1008.1511.

[12] M. Abramowitz and I. A. Stegun. *Handbook of Mathematical Functions with Formulas, Graphs, and Mathematical Tables*. 10th ed. United States Department of Commerce, National Bureau of Standards; Dover Publications, 1972.

[13] Kalliopi Petraki, Marieke Postma, and Jordy de Vries. “Radiative bound-state-formation cross-sections for dark matter interacting via a Yukawa potential”. In: (2016). arXiv: 1611.01394v2.

[14] Michael A. Stroscio. “Positronium: A review of the theory”. In: *Physics Reports* 22 (1975).

[15] R.L. Greene and C. Aldrich. “Variational Wave Functions for a Screened Coulomb Potential”. In: *Physics Review A* 14 (1976), pp. 2363–2366. DOI: 10.1103/PhysRevA.14.2363.

[16] Sebastian Cassel. "Sommerfeld factor for arbitrary partial wave processes". In: (2009). arXiv: 0903.5307v1.